

Online Algorithms and Policies Using Adaptive and Machine Learning Approaches*

Anuradha M. Annaswamy[†], Anubhav Guha, Yingnan Cui,
Joseph E. Gaudio[‡] and José M. Moreu

Abstract

This paper considers the problem of real-time control and learning in dynamic systems subjected to uncertainties. Adaptive approaches are proposed to address the problem, which are combined with methods and tools in Reinforcement Learning (RL) and Machine Learning (ML). Algorithms are proposed in continuous-time that combine adaptive approaches with RL leading to online control policies that guarantee stable behavior in the presence of parametric uncertainties that occur in real-time. Algorithms are proposed in discrete-time that combine adaptive approaches proposed for parameter and output estimation and ML approaches proposed for accelerated performance that guarantee stable estimation even in the presence of time-varying regressors, and for accelerated learning of the parameters with persistent excitation. Numerical validations of all algorithms are carried out using a quadrotor landing task on a moving platform and benchmark problems in ML. All results clearly point out the advantage of the proposed integrative approaches for real-time control and learning.

1 Introduction

The primary goal of this paper is the real-time control of dynamic systems that are subject to uncertainties and a secondary goal is to learn the uncertainties. Methods for realizing these goals abound in the controls community, examples of which include adaptive control [1–7], robust control [8,9], model-predictive control [10,11], and sliding-mode control [12]. A more recent entrant into this area is reinforcement learning (RL), a subfield of Machine Learning (ML), which has been proposed for the development of control policies for complex systems and environments [13–17]. The secondary goal has also been addressed at length by the control community in the case when the uncertainties are parametric in nature [18–20] with a focus on deriving accurate estimates of parameters, states, and outputs using underlying dynamic models. Similarly there has been a concerted effort in the ML community where the goal is to achieve an accelerated reduction of a loss function through an iterative adjustment of its minimizer [21–24].

*This work is supported by the Boeing Strategic University Initiative and the Air Force Research Laboratory, Collaborative Research and Development for Innovative Aerospace Leadership (CRDInAL), Thrust 3 - Control Automation and Mechanization grant FA 8650-16-C-2642.

[†]AMA, AG, YC, and JM are with MIT, Cambridge, MA, 02139

[‡]JEG is with Aurora Flight Sciences, a Boeing Company, Cambridge MA 02140

The field of adaptive control (AC) has always included as a central element in its design a parametric learning component. With the starting point as the control of a dynamic system whose uncertainties are parametric, the adaptive control solution has consisted of a control input that explicitly includes a parameter estimate which is recursively adjusted using all available data in real-time so as to converge to its true value. The overall goal of the adaptive system is to guarantee that the control input results in the closed-loop adaptive system to have globally bounded solutions, with a secondary goal of learning the true parameter, which completely coincides with the primary and secondary goals mentioned above. With adaptation to parametric uncertainties as the key architecture of the controller, robustness to nonparametric uncertainties such as time-variations in parameters and unmodeled dynamics have been ensured through regularization and persistent excitation [25, 26]. The field of ML has as its goal the determination of a sequence of inputs that drives a dynamical system to maximize a suitable objective with minimal knowledge of the system model. The central structure of the RL solution revolves around a policy that is learned so as to maximize a desired reward [13, 16]. This policy is often parameterized in the form of a neural network, and an offline recursive update of the weights that ensures convergence is then addressed [14, 17].

Both AC and RL methods that have been designed for control have addressed the problem of control in the presence of uncertainty, with the component of learning addressed explicitly. The two however have deployed entirely different approaches for accomplishing this objective. AC methods have been proven to be effective in a “zero-shot” enforcement of control objectives for specific classes of problems, that is, in learning to accomplish a task online [1, 2, 13, 27]. These adaptive techniques are able to accommodate, in real-time, parametric uncertainties and constraints on the control input magnitude [28, 29] and rate [30]. Despite these abilities to accommodate the presence of modeling errors over short time-scales and meet tracking objectives, AC methods are unable to directly guarantee the realization of long-term optimality-based objectives. RL-trained policies, on the other hand, can handle a broad range of objectives [31], where the control policies are learned largely in simulation. Training in simulation is a powerful technique, allowing for a near infinite number of agent-environment interactions to allow the policy to become optimal. In practice, however, offline policies trained in simulation often exhibit degenerate performance when used for real-time control due to modeling errors that can occur online [32, 33]. It may be difficult to reliably predict the behavior of a learned policy when it is applied to an environment different from the one seen during training [34–37]. The first set of approaches we propose in this paper seeks to bridge this “sim-to-real” gap by proposing various combinations of the AC and RL approaches so as to realize their individual advantages and minimize their weaknesses.

In the context of the secondary goal of learning the uncertainty, a particular body of work in ML has focused on accelerated convergence of an underlying cost function and the associated accelerated learning of the minimizer of this function (see for example, [21–24, 38]). These pertain to the use of higher-order iterative momentum-based update algorithms which have seen widespread applications in training machine learning models [39, 40]. Such methods have only considered the case when regressors, which are exogenous, are static. Several physical systems are routinely subjected to dynamics which can cause these regressors to be time-varying. AC methods such as [18–20, 41, 42] and recent results in [43–45] have precisely focused on these cases, leading to stability by employing normalization and parameter convergence using persistent excitation. The second set of approaches that we present in this paper seeks to combine the stability-based perspective in AC with the accelerated learning-based perspective in ML and realize both of their advantages.

We present two classes of AC-ML algorithms, the first in continuous time, and the second in discrete-time. In the first class, the combination is that of AC and RL, and is based on the time-scales of decision-making, with AC-based components in the inner-loop and RL-based ones in the outer-loop. We propose three different algorithms, which employ three different update rules for adjusting the control parameters in real-time in the inner-loop, denoted as AC-RL, HTAC-RL, and MSAC-RL, with emphasis on real-time control. While the first group of AC-RL accommodates parametric uncertainties, the second departs from a standard gradient descent approach and allows the potential of an accelerated performance through high-order tuners. The MSAC-RL algorithm accommodates magnitude constraints of control inputs. The role of RL in each case is to train through simulation the optimal control needed to maximize a desired objective, where the simulation is assumed to have access to a reference system that is the best plant-model available. With a judiciously chosen control input that combines the two methods and adaptive laws determined by each of the three algorithms for updating the control parameters, the resulting closed-loop system is proved to be stable for a class of nonlinear plant-models with certain parametric uncertainties. A Lyapunov approach is employed for this purpose. The performance of the algorithms is quantified through closed-loop stability and Regret [46,47], defined as the difference in control performance between the controller employing a given algorithm and the best controller given full knowledge of the plant. All validations and comparisons are carried out using a numerical experiment of a quadrotor that is required to land on a moving platform, with high-fidelity models that include realistic mechanisms of nonlinear kinematics, actuator nonlinearities, and measurement noise. While state variables are assumed to be accessible for the problems addressed in this class and that the nonlinear systems are feedback linearizable, extensions to more general nonlinear systems such as those in [5, 47, 48] can be carried out in a straight forward manner.

The second class of AC-ML algorithms that we propose in this paper is in discrete-time, where the emphasis is on prediction and estimation, with goals of accelerated performance measured via a loss function and accelerated learning. Here, the combination of AC and ML is at the algorithmic level, where concepts from both fields are integrated to generate new algorithms. The AC-ML algorithms we propose in this second class show that stability can be achieved even with time-varying regressors, and with additional properties of accelerated performance. Building on the recent results established in [49,50], these algorithms are shown to be robust to noise and disturbances [51], to be applicable to general loss functions that are convex [52], and to have non-asymptotic convergence rates that are a log-factor away from Nesterov’s algorithms in [38] under comparable conditions. In addition to algorithms that achieve accelerated performance, we also propose algorithms that achieve accelerated learning of the parameters. For this purpose, we will leverage conditions of persistent excitation [41, 53, 54].

Efforts to combine AC and ML approaches have been highlighted in several recent works, which include [47, 55–58]. Other than our earlier work in [49, 50], new algorithms that combine AC and RL in continuous-time systems can be found in [59–61]. [59] proposes the use of adaptive control for nonlinear systems in a data-driven manner, but requires offline trajectories from a target system and does not address accelerated learning or magnitude saturation. References [60,61] study the linear-quadratic-regulator problem and its adaptive control variants from an optimization and machine learning perspective. In [57] a reinforcement learning approach is used to determine an adaptive controller for an unknown system, while in [58] principles from adaptive control and Lyapunov analysis are used to adjust and train a deep

neural network. For the second class of algorithms in discrete-time, other than our earlier work in [50–52], to our knowledge, similar combinations of AC and ML for accelerated performance and convergence have not been reported to-date.

The contributions of the paper are the following:

- A suite of algorithms in continuous-time that combine AC and RL approaches that lead to online control policies that guarantee stable behavior in the presence of parametric uncertainties that occur in real-time. Three algorithms, AC-RL, HTAC-RL, and MSAC-RL are presented, with stability and performance guarantees for a class of continuous nonlinear systems. Numerical validation is carried out using an example of a quadrotor required to land on a moving platform when subjected loss of control effectiveness and parametric uncertainties mid-flight.
- A suite of algorithms in discrete-time that combine adaptive approaches proposed for parameter and output estimation and ML approaches proposed for accelerated performance that guarantee stable estimation even in the presence of time-varying regressors, and for accelerated learning of the parameters with persistent excitation. Numerical validation is carried out using benchmark problems in ML.

Preliminary versions of the results reported here can be found in peer-reviewed publications [50] and [52], and arXived publications [51, 62, 63]. Section 3 is a significant expansion of [62] which only addressed the single-input version of the result in Section 3.1. Section 4 is a significant expansion of [50] and [52], includes a comprehensive treatment of accelerated performance as well as accelerated learning in comparison to [51, 63], and illustrates the central contribution of the corresponding algorithms and improvements compared to standard adaptive and ML approaches.

In Section 2, we state the problems that correspond to the primary and secondary goals of the paper. In each case, the state-of-the-art approaches in AC and ML are described. In Section 3, on-line policies for solving the control problem are described, which correspond to the first contribution of the paper. Section 4 articulates the second contribution, which pertain to on-line algorithms for accelerated performance and accelerated learning. Section 5 includes a summary and concluding remarks. Proofs of all theorems can be found in the appendix.

2 Problem Statement

The two problems that we address in this paper pertain to control and learning, and are addressed separately in Sections 2.1 and 2.2. The treatment is in continuous-time in Section 2.1 and in discrete-time in Section 2.2 as these formulations are most appropriate for the underlying goals.

2.1 The online control problem

Consider a continuous-time, deterministic nonlinear system described by the following dynamics:

$$\dot{X}(t) = f(X(t), U(t)) \tag{1}$$

where $X(t) \in \mathbb{R}^n$, and $U(t) \in \mathbb{R}^m$. We consider the system behavior around an equilibrium point (X_0, U_0) , and rewrite (1) as

$$\dot{x} = Ax + Bu + h(x, u) \quad (2)$$

where $x = X - X_0$, $u = U - U_0$, $A = \nabla_x f(X_0, U_0)$, $B = \nabla_u f(X_0, U_0)$ and $h(x, u)$ represents higher order residual terms. The problem that we address is the determination of the control input $u(t)$ in (2) in real-time, when parametric uncertainties are present in one or more of the components A , B , and $h(x, u)$. The goal is to choose u so as to minimize a suitable cost function of x and u , which is stated as

$$\begin{aligned} \min_{u(t) \in U \forall t \in [0, T]} & \int_0^T c(x(t), u(t)) dt \\ \text{subject to} & \text{ Dynamics in (2) } \forall t \in [0, T] \\ & x(0) = x_0 \end{aligned} \quad (3)$$

for a given initial condition x_0 .

2.1.1 The Classical Online Approach Based on Adaptive Methods

The general problem of determining u in (2) so that $x(t)$ behaves in a desired manner has been considered at length in the adaptive control literature. In what follows, we focus on a specific class of such systems with parametric uncertainties for which we propose a new solution. This class is summarized in the following three assumptions:

Assumption A1: The residue $h(x, u)$ is of the form

$$h(x, u) = B\Theta_{nl}^* \phi(x) \quad (4)$$

where $\phi(x(t)) \in \mathbb{R}^l$ is a known nonlinear function and $\Theta_{nl}^* \in \mathbb{R}^{m \times l}$ is an unknown parameter matrix.

Assumption A2: A and B are such that $\Theta_l^* \in \mathbb{R}^{m \times n}$ exists such that

$$A + B\Theta_l^* = A_H \quad (5)$$

where A_H is a known Hurwitz matrix.

Assumption A3: The uncertainties in B are such that

$$B = B_r \Lambda^* \quad (6)$$

where $B_r \in \mathbb{R}^{n \times m}$ is known, but $\Lambda^* \in \mathbb{R}^{m \times m}$ is unknown, and satisfies the assumption

$$\Lambda^{*T} S + S^T \Lambda^* \text{ is positive-definite.} \quad (7)$$

where S is a known matrix.

Remark 1. *Assumption A1 implies that the nonlinearities lie in a subspace spanned by the input-matrix. Several positioning systems such as inverted pendulums [62], quadrotors [64], and several other flight platforms [65] satisfy such an assumption. Assumption A2 is akin to controllability, often referred to as a matching condition, is required for adaptive state-feedback problems, as it guarantees the existence of a solution that specifies the desired behavior from*

the closed-loop system when there are no parametric uncertainties. This too is satisfied by several positioning systems and flight platforms [65]. Finally Assumption A3 is a requirement in adaptive control [41] related to directional information in the control matrix. Λ^* can be viewed as a loss of effectiveness of the actuator, with its nominal value $\Lambda_r = I$. A simple example is the case when Λ^* is a diagonal matrix whose entries have a known sign, which allows S to be chosen to be diagonal with entries that are either +1 or -1 to satisfy (7). The numerical example we will discuss in Section 3.4 includes uncertainties that meet all three assumptions.

The classical adaptive control solution for the control of (2), subject to Assumptions A1-A3 is given by

$$u(t) = K(t)r(t) - \Theta_{nl}(t)\phi(x(t)) + \Theta_l(t)x(t) \quad (8)$$

$$\dot{K}(t) = -\Gamma_K B_r^T P e(t) r^T(t) \quad (9)$$

$$\dot{\Theta}_{nl}(t) = \Gamma_{\Theta_{nl}} B_r^T P e(t) \phi^T(x(t)) \quad (10)$$

$$\dot{\Theta}_l(t) = -\Gamma_{\Theta_l} B_r^T P e(t) x^T(t) \quad (11)$$

where $\Gamma_K, \Gamma_{\Theta_{nl}}, \Gamma_{\Theta_l}$ are positive-definite, P is the symmetric and positive definite solution to the Lyapunov equation

$$PA_H + A_H^T P = -Q \quad (12)$$

for a given symmetric positive definite matrix Q . $r(t)$ is an exogenous reference input specified such that it generates a desired signal $x_r(t)$ that the plant state $x(t)$ should follow. This reference model is chosen as

$$\dot{x}_r(t) = A_H x_r(t) + B_r r(t) \quad (13)$$

which specifies the desired behavior from the plant when there are no parametric uncertainties present, and $e(t) = x(t) - x_r(t)$. That is, $e(t)$ represents a performance error for the closed-loop adaptive system. It can be shown that under Assumptions A1-A3, the closed-loop system specified by (2) and the adaptive controller in (8)-(13) has globally bounded solutions and that $\lim_{t \rightarrow \infty} e(t) = 0$ [1]. Similar to [55], we define Regret using the performance error e as

$$\mathcal{R} = \int_0^T e^T(\tau) Q e(\tau) d\tau. \quad (14)$$

It is clear that for the classical AC approach, $\mathcal{R} = O(1)$. As in [55], decaying exponential signals can be included in (14) as well.

2.1.2 An Offline Approach Based on Reinforcement Learning

Control policies are determined using RL through offline training in simulation, which implies that the system in (2) needs to be fully known during the offline training. The system that is used for training is denoted as a reference system which can be described as

$$\dot{x}_r = Ax_r + Bu_r + h(x_r, u_r) \quad (15)$$

in which the subscript r denotes signals and parameters belonging to the reference system. In order to lead to a self-contained exposition, we briefly describe the RL training procedure.

First, it is assumed that continuous-time dynamics in (15) is sampled with sufficient accuracy, resulting in the discrete time dynamics:

$$x_{r,k+1} \sim p(x_{r,k+1}|x_{r,k}, u_{r,k}) \quad (16)$$

where p represents the state transition probability. An appropriate numerical integration scheme ensures that this discrete-time formulation closely approximates the dynamics. When training in simulation the RL process begins with the construction of a simulation environment defined by (16). The reference system in (15) is used to collect data with which RL learns a feedback policy $u_r(t) = \pi(x_t)$ with repeated training of $\pi(\cdot)$ so as to achieve the control objective of (3) [66] as follows.

At each timestep, an observation $x_{r,k}$ is received, a control $u_{r,k}$ is chosen, and the resulting cost c is received. Repeating this process, a set of input-state-cost tuples $\mathcal{D} = [(x_{r,1}, u_{r,1}, c_1), \dots, (x_{r,N}, u_{r,N}, c_N)]$ are formed. This data is used to train and update π . In typical RL algorithms the policy is parametrized, so that $u_k \sim \pi_\theta(x_k)$. For example, in deep RL θ represents the weights/biases of a neural network. The learning algorithm then seeks to adjust θ so that the expected accumulated cost is minimized [16, 67], i.e

$$\min_{\theta} J(\theta) = \mathbb{E}_{\pi_\theta} \left[\sum_{k=0}^T c_k \right] \quad (17)$$

The policy gradient can be calculated as:

$$\nabla_{\theta} J(\theta) = \mathbb{E} \left[- \sum_{k=0}^T A^{\pi_\theta}(x_k, u_k) \nabla_{\theta} \log \pi_{\theta}(u_k|x_k) \right] \quad (18)$$

where A^{π_θ} is the advantage function [67]. A gradient descent-based approach is then used to update θ . The reader is referred to [67] for further details on policy gradients.

Though the above RL approach has led to compelling successes, analytical guarantees of convergence to optimal policies have been shown only in simple settings. For example, if the state and action spaces are discrete with $x_k \in \mathbb{X}$, $u_k \in \mathbb{U} \forall k$ for finite sets \mathbb{X} , \mathbb{U} , Watkin's Q -learning algorithm can be used to achieve the globally optimal policy. The corresponding optimal Q function is given by the fixed point solution to the Bellman equation:

$$Q^*(x, u) = -c(x, u) + \gamma \sum_{x' \in \mathbb{X}} p(x'|x, u) \max_{u' \in \mathbb{U}} Q^*(x', u') \quad (19)$$

where $0 < \gamma < 1$ is a discount factor leading to a corresponding optimal policy $\pi^*(x) = \operatorname{argmax}_{u \in \mathbb{U}} Q^*(x, u)$. An iterative rule for determining the optimal Q -function, denoted as Q -learning, is given by

$$\hat{Q}(x_k, u_k) \leftarrow \hat{Q}(x_k, u_k) + \eta_k \delta_k \quad (20)$$

where η_k is a sequence of learning rates, and $\delta_k = -c_k + \gamma \max_{u' \in \mathbb{U}} \hat{Q}(x_{k+1}, u') - \hat{Q}(x_k, u_k)$ is the temporal difference error [16, 17]. If η_k satisfies the Robbins-Monro conditions and every state-action pair is visited infinitely often, then the Q function estimate converges to the fixed-point solution: $\hat{Q}(x, u) \rightarrow Q^*(x, u) \forall x \in \mathbb{X}, u \in \mathbb{U}$ [17].

Remark 2. *Two important assumptions are required by RL to provide these guarantees of convergence. The first assumption is that the transition probabilities in (16) do not change during the Q-learning process. Therefore, that (16) has no parametric uncertainties is a requirement for the convergence result. The second assumption is that \mathbb{X} and \mathbb{U} are finite sets. In several physical systems, the state and action spaces are continuous, which makes the finite-set assumption restrictive. Any discretization therefore necessarily leads to an approximate optimization of the cost function in (3). It should be noted that a huge body of literature exists in RL that attempt to relax these assumptions [68–70]. The approach that we delineate in Section 3 is distinct from these methods.*

2.2 The online learning problem

The second problem that we consider pertains to

$$y_k = - \sum_{i=1}^n a_i^* y_{k-i} + \sum_{j=1}^m b_j^* u_{k-j-d} + \sum_{\ell=1}^p c_\ell^* f_\ell(z_{k-1}^T, v_{k-d-1}^T) + \eta_k, \quad (21)$$

which represents a single-input, single-output system with input u_k and output y_k , where a_i^* , b_j^* and c_ℓ^* are unknown parameters that need to be identified, d is a known time-delay, $z_{k-1} = [y_{k-1}, \dots, y_{k-n}]^T$ and $v_{k-d-1} = [u_{k-1-d}, \dots, u_{k-m-d}]^T$. The function f_ℓ is an analytic function of its arguments and is assumed to be such that the system in (21) is bounded-input-bounded-output stable. $\{\eta_k\}$ is a stochastic process on probability space $(\Omega, \mathcal{F}, \mathbb{P})$ and η_k satisfies

$$E(\eta_{k+1} | \mathcal{F}_k) = d_{k+1} \text{ a.s.} \quad (22)$$

$$E(\eta_{k+1}^2 | \mathcal{F}_k) = \sigma_{k+1}^2 \text{ a.s.} \quad (23)$$

where \mathcal{F}_k is a filtration on the sub-sigma increasing algebra group of $\sigma_k(\theta_1, \vartheta_1, \dots, \theta_k, \vartheta_k)$ (i.e., the filtration \mathcal{F}_k assumes we know all values of θ_i and ϑ_i , $\forall i \leq k$) [71]. The goal is to determine a predictor \hat{y}_k that accurately estimates y_k as well as to estimate the unknown parameters. In what follows, we assume that u_k is a bounded function for all k .

We rewrite (21) in the form of a linear regression

$$y_k = \phi_{k-1}^T \theta^* + \eta_k, \quad (24)$$

where

$$\phi_{k-1} = [z_{k-1}^T, v_{k-d-1}^T, f_1(z_{k-1}^T, v_{k-d-1}^T), \dots, f_p(z_{k-1}^T, v_{k-d-1}^T)]^T \quad (25)$$

is a regressor determined by the input u_k and $\theta^* = [a_1^*, \dots, a_n^*, b_1^*, \dots, b_m^*, c_1^*, \dots, c_\ell^*]^T$ is the unknown parameter vector. The focus of this section is to learn the parameter θ^* using a recursive estimator

$$\hat{y}_k = \phi_{k-1}^T \theta_{k-1}. \quad (26)$$

Defining

$$e_{y,k} = \hat{y}_k - y_k, \quad (27)$$

and a loss function

$$L_k = \frac{1}{2} e_{y,k}^2, \quad (28)$$

the convergence of the loss function L_k to zero is defined as the performance goal, while the convergence in parameter, of θ_k to θ^* is defined as the learning goal. Two goals of interest here are accelerated performance and accelerated learning.

2.2.1 Adaptive approaches to performance and learning

The standard approach for achieving the performance goal is based on an iterative normalized gradient descent method (see for example, [19]) which employs $\nabla_{\theta} L_k$. From (26) and (27), it follows that

$$\nabla_{\theta_{k-1}} L_k = \phi_{k-1} e_{y,k}. \quad (29)$$

The update with a normalized gradient is of the form

$$\theta_k = \theta_{k-1} - \Gamma \frac{\nabla_{\theta_{k-1}} L_k}{\mathcal{N}_{k-1}}, \quad 0 < \gamma < 2 \quad (30)$$

where Γ is a gain matrix, and \mathcal{N}_k is a suitable normalization, an example of which is $1 + \phi_k^T \phi_k$. In order to realize the learning goal, of convergence of θ_k to θ^* , the following property of excitation of the regressor ϕ_k is needed [19, 42, 63]. We denote \mathbb{N}^+ as the set of positive integers, and $\|\cdot\|$ as the Euclidean norm.

Definition 1 ([72]). *A bounded function $\phi_k : [k_0, \infty) \rightarrow \mathbb{R}^N$ is persistently exciting (PE) at a level α if there exists $\Delta T \in \mathbb{N}^+$ and $\alpha > 0$ such that*

$$\sum_{i=k+1}^{k+\Delta T} \phi_i \phi_i^T \succeq \alpha I, \quad \forall k \geq k_0.$$

When the regressors in (25) satisfy the PE condition, it can be shown using the methods in [19, 42, 63] that θ_k converges to θ^* uniformly in k . We note that if the gain matrix in (30) is time-varying and updated as

$$\Gamma_{k-1} = \Gamma_{k-2} - \frac{\Gamma_{k-1} \phi_{k-1} \phi_{k-1}^T \Gamma_{k-1}}{1 + \phi_{k-1}^T \Gamma_{k-2} \phi_{k-1}}, \quad (31)$$

with \mathcal{N}_{k-1} in (30) being $1 + \phi_{k-1}^T \Gamma_{k-2} \phi_{k-1}$, we have the well-known least squares algorithm [54, p. 58].

2.2.2 ML approaches to accelerated performance

A seminal paper was written thirty years ago in [38] and subsequently expanded on recently in [22–24] and several others with a focus on accelerated performance, i.e. fast convergence of L_k to zero with k . This Nesterov’s algorithm is of the form

$$\theta_k = \nu_{k-1} - \bar{\alpha} \nabla f(\nu_{k-1}) \quad (32)$$

$$\nu_k = (1 + \bar{\beta}) \theta_k - \bar{\beta} \theta_k \quad (33)$$

where the normalized loss function f is defined as

$$f_k(\theta_{k-1}) = \frac{L_k}{\mathcal{N}_{k-1}} + \frac{\mu}{2} \|\theta_{k-1} - \theta_0\|^2, \quad \mu > 0 \quad (34)$$

and L_k was assumed to be continuously differentiable, smooth and convex, with a smoothness parameter \bar{L} , $\bar{\alpha}$ is a function of \bar{L} , and $\bar{\beta}$ may be chosen as a function of k . A convergence rate of $\mathcal{O}(1/k^2)$ was established in [38] for the specific case when L_k only varied with the parameter estimate, but otherwise did not vary as a function of k . Equations (26)-(28) imply in turn that the underlying regressor ϕ_k is a constant, which rarely occurs in dynamic systems. Our focus in this section is to realize the property of accelerated performance of Nesterov’s algorithm for the case when ϕ_k varies with k as in (25).

3 Online Control Policies - Continuous-time

3.1 AC-RL

We return to the plant model in (2), which when subjected to Assumptions *A1-A3*, is of the form

$$\dot{x} = Ax + B_r \Lambda^*(u + \Theta_{nl}^* \phi(x)) \quad (35)$$

where B_r is known, and $\phi(x), x$ are measurable. This plant-model is subjected to parametric uncertainties, i.e, the parameters Θ_{nl}^* , Θ_l^* and Λ^* are unknown. Additionally, Θ_l^* satisfies Assumption *A2*, and Λ^* satisfies (7). We next introduce the reference system which will be used for training the RL. When there are no parametric uncertainties in (35), i.e, $\Theta_l^* = \Theta_{l,r}$, $\Theta_{nl}^* = \Theta_{nl,r}$ for known $\Theta_{l,r}, \Theta_{nl,r}$, the reference system in (15) becomes

$$\dot{x}_r = Ax_r + B_r(u_r + \Theta_{nl,r} \phi(x_r)) \quad (36)$$

where we have used the fact that $\Lambda_r = I$.

Assumption A4: A control input $u_r(t)$ for the system in (36) can be determined using RL methods such that the cost function in (3) is approximately minimized when $u(t) = u_r(t)$, $\Theta_l^* = \Theta_{l,r}$, $\Theta_{nl}^* = \Theta_{nl,r}$, $\Lambda^* = I$, and $x(t)$ is bounded for all initial conditions $x(0)$.

It should be noted that the approximate minimization from $u_r(t)$ in Assumption *A4* is essentially due to the accuracy of the training using discretized data. Assumption *A4* implies that u_r implicitly generates a signal such that the nonlinear system (36) remains stable, and generates solutions that are well behaved and optimal. One possible method by which such a u_r can be generated is given by

$$u_r(t) = u_{\text{exog}}(t) - \Theta_{nl,r} \phi(x_r(t)) + \Theta_{l,r} x_r(t) \quad (37)$$

where $\Theta_{l,r}$ is such that $A_H = A + B_r \Theta_{l,r}$ is a Hurwitz matrix. We summarize this in the form of Assumption *A4'*:

Assumption A4': $u_r(t)$ generated by the RL method is of the form (37), where u_{exog} is a bounded signal.

It should be noted that this reference system in (36) is an implicit description. The value of $x_r(t)$ is determined using data obtained from simulations from RL as described in Section 2.1.2 with an input $u_r(t)$ into the simulation-model of the true system with nominal parameters. The structure of $u_r(t)$ as in (37) is an implicit one, which will be used for stability analysis and not for realization of the RL-input $u_r(t)$.

We now describe the AC-RL algorithm:

$$u = K(t)u_{\text{exog}}(t) - \Theta_{nl}(t)\phi(x) + \Theta_l(t)x(t) \quad (38)$$

$$\dot{K} = -\Gamma_K B_r^T P e(t) u_{\text{exog}}^T(t) \quad (39)$$

$$\dot{\Theta}_{nl} = \Gamma_{\Theta_{nl}} B_r^T P e(t) \phi^T(x(t)) \quad (40)$$

$$\dot{\Theta}_l = -\Gamma_{\Theta_l} B_r^T P e(t) x^T(t) \quad (41)$$

In (38)-(41), $e(t) = x(t) - x_r(t)$, $K(t)$ and $\Theta_{nl}(t), \Theta_l(t)$ are adaptive parameter estimates, $\Gamma_K, \Gamma_{\Theta_{nl}}, \Gamma_{\Theta_l}$ are positive definite matrices, and P is given by (12). $u_{\text{exog}}(t)$ can be determined using $u_r(t), x_r(t)$, and (37) as $\phi(x)$ is a known function of x . It is clear from (39) - (41) that if there are no parametric uncertainties, and if the initial conditions of (35) are identical to those

of (36), with $K(0) = I$, $\Theta_{nl}(0) = \Theta_{nl,r}$ and $\Theta_l(0) = \Theta_{l,r}$, then the AC-RL policy coincides with $u_r(t)$. For the rest of this paper, unless otherwise mentioned, we choose $Q = 2I$. The following theorem presents the stability property of the AC-RL as well as Regret (defined in (14)):

Theorem 1. *Under Assumptions A1-A3 and A4', the closed-loop systems specified by the target system (35), the reference system (36), and the AC-RL controller given by (38) - (41) will have globally bounded solutions, with $\lim_{t \rightarrow \infty} \|e(t)\| = 0$, with $\mathcal{R} = O(1)$.*

3.2 HTAC-RL

Rather than the gradient-descent based adaptive laws in (39)-(41), we propose a high-order tuner (HT), starting from a dynamic loss function [49]

$$L_t = \frac{d}{dt} \left\{ \frac{e^T P e}{2} \right\} + \frac{e^T Q e}{2}. \quad (42)$$

Defining $\Theta = [K, \Theta_{nl}, \Theta_l]$ and $\omega = [u_{\text{exog}}^T, -\phi^T, x^T]^T$, the HT is of the form

$$\begin{aligned} \dot{\Xi} &= -\gamma B_r^T P e \omega^T \\ \dot{\Theta} &= -\beta(\Theta - \Xi) \mathcal{N}_t, \end{aligned} \quad (43)$$

where

$$\mathcal{N}_t = 1 + \mu \omega^T \omega \quad (44)$$

$$\mu \geq \frac{2\gamma}{\beta} \|P B_r\|_F^2 \quad (45)$$

where $\|\cdot\|_F$ in (45) denotes the Frobenius matrix norm. We replace (7) with the following more restrictive assumption on the input uncertainty for this algorithm:

Assumption A5: Λ^* is symmetric and positive definite, with $\|\Lambda^*\| \leq 1$.

Theorem 2. *Under Assumptions A1-A2, A4', and A5, the closed-loop adaptive system specified by (35), (36), (38) and (43) has globally bounded solutions with $\lim_{t \rightarrow \infty} e(t) = 0$ with $\mathcal{R} = O(1)$.*

It should be noted that (43) is a second-order tuner, and an extension of our earlier results in [49] to the multivariable case. The update of the intermediate parameter estimate Ξ differs from the gradient of the loss function ∇L_t , as the latter includes the input matrix Λ^* which is unknown. A second point to note is the replacement of *Assumption A3* with the more restrictive *A5*, introduced due to the presence of multiple inputs. As Λ^* typically denotes a loss of effectiveness of the controller, bounding its norm by unity is a reasonable assumption.

3.3 MSAC-RL

As control inputs are often subject to magnitude saturation, we propose yet another variation, Magnitude Saturation AC-RL (MSAC-RL), which builds on the ideas introduced in [28]. The saturated control input into the true plant is calculated as:

$$u_i(t) = u_{i,\text{max}} \text{sat} \left(\frac{u_{i,c}(t)}{u_{i,\text{max}}} \right) \quad (46)$$

where $u_c(t)$ denotes the output of the controller. This induces a saturation-triggered disturbance Δu vector defined by

$$\Delta u(t) = u_c(t) - u(t) \quad (47)$$

It is easy to see that $\Delta u(t) = 0$ when the desired control $u_c(t)$ does not saturate. The output of the controller, u_c , is given by:

$$u_c = K(t)u_{\text{exog}}(t) + \Theta_l(t)x(t) - \Theta_{nl}(t)\phi(x(t)) \quad (48)$$

We introduce a new performance error e_a in order to accommodate the disturbance Δu as follows:

$$\dot{e}_a = A_H e_a + B_r K_a \Delta u \quad (49)$$

which leads to a new augmented error $e_u = e - e_a$:

$$\dot{e}_u = A_H e_u + B_r \Lambda^* \left[\tilde{K}(t)u_{\text{exog}}(t) + \tilde{\Theta}_l^T(t)x(t) - \tilde{\Theta}_{nl}^T(t)\phi(x(t)) \right] + B_r (\Lambda - K_a^T) \Delta u \quad (50)$$

This suggests a different set of adaptive laws, where all Γ_i s are positive definite:

$$\begin{aligned} \dot{K} &= -\Gamma_K B_r^T P e_u u_{\text{exog}}^T, & \dot{K}_a &= \Gamma_a B_r^T P e_u \Delta u^T \\ \dot{\Theta}_{nl} &= \Gamma_{nl} B_r^T P e_u \phi^T(x), & \dot{\Theta}_l &= -\Gamma_l B_r^T P e_u x^T \end{aligned} \quad (51)$$

Theorem 3. *Under Assumptions A1-A3 and A4', the closed-loop adaptive system specified by the target system (35), the reference system (36), the magnitude constraint in (46) and the MSAC-RL controller given by (48)-(51) will*

- (i) *have globally bounded solutions, with $\lim_{t \rightarrow \infty} \|e_u(t)\| = 0$ if the target system in (35) is open-loop stable.*
- (ii) *have bounded solutions for all initial conditions $x(0)$, $K(0)$, $\Theta_{nl}(0)$, $\Theta_l(0)$ and $K_a(0)$ in a bounded domain, with $\|e(t)\| = O[\int_0^t \|\Delta u(\tau)\| d\tau]$ if the target system in (35) is not open-loop stable.*

Remark 3. *The choice of the control input in the three algorithms above as in (38) is very similar to that in the classical AC approach in (8). The latter does not address how the reference signal $r(t)$ is generated, leaving it to other methods based on trajectory generation. Our contribution lies in identifying the role of RL in this context and suitably integrating it into the AC methodology. As is apparent from (38), the overall control is not a direct addition of the two components but suitably combined, and utilizing only a part of u_r , which is generated by RL, in the parameter update laws.*

Remark 4. *All three algorithms presented in Section 3 combine AC approaches with RL approaches, where the AC components are introduced in the inner-loop and provide the fast and necessary correction in real-time, with the focus on the primary goal of ensuring control performance, while the RL approaches based on policy gradients such as the Proximal Policy Optimization (PPO) algorithm from [73] are used in an outer-loop to accommodate continuous state and action spaces with the focus on the secondary goal of learning. The HTAC-RL algorithm strives to have an accelerated performance, while the MSAC-RL algorithm expands the scope of the AC approach to include the ubiquitous limits present on the control input magnitude. Extensions of the latter that accommodates rate-limits can be carried out in a similar manner using the approaches outlined in [30].*

It is clear that the performance guarantees of the closed-loop system in Theorems 1-3 approximate the online control goal stated in (3) for the case when the cost function does not depend on the control input, as $x(t)$ approaches $x_r(t)$ and the choice of $u_r(t)$ optimizes the behavior of the reference system. Any dependence on the control input is implicitly addressed in MSAC-RL by accommodating magnitude saturation. More remains to be done in bridging this optimization gap, a topic for future research.

3.4 Numerical Validation of the AC-RL, MSAC-RL, and HTAC-RL architectures

We validate the proposed AC-RL, HTAC-RL and MSAC-RL on a simulated task, in which an autonomous quadrotor must land on a moving platform. PPO is used to train a control policy in simulation, which is then utilized at the outer loop of the various adaptive control algorithms.

3.4.1 Quadrotor Dynamics

We first describe the quadrotor dynamical model. The squared angular velocities of each propeller are used as input, that is: $u = [\omega_1^2, \omega_2^2, \omega_3^2, \omega_4^2]^T$. The thrust produced by each propeller is calculated by multiplying the squared angular speed by a propeller specific constant κ . Letting $K = \text{diag}(\kappa_1, \kappa_2, \kappa_3, \kappa_4)$, the vector of thrusts produced by each propeller is then given by Ku . Finally, denoting the (body-frame) vertical force, roll moment, pitch moment, and yaw moment by $f_z, \tau_\phi, \tau_\theta, \tau_\psi$ respectively, we have:

$$\begin{bmatrix} f_z \\ \tau_\phi \\ \tau_\theta \\ \tau_\psi \end{bmatrix} = \begin{bmatrix} 1 & 1 & 1 & 1 \\ L & 0 & -L & 0 \\ 0 & L & 0 & -L \\ \mu & -\mu & \mu & -\mu \end{bmatrix} Ku \quad (52)$$

where L is the distance from each propeller to the quadrotor center of mass, and μ is a rotational drag constant. Assuming low-speeds, we may then construct a simple rigid-body model for the quadrotor dynamics:

$$\begin{aligned} \ddot{x} &= (\cos \phi \cos \theta \cos \psi + \sin \phi \sin \psi) \frac{f_z}{m} \\ \ddot{y} &= (\cos \phi \sin \theta \sin \psi - \sin \phi \cos \psi) \frac{f_z}{m} \\ \ddot{z} &= \cos \phi \cos \theta \frac{f_z}{m} - g \\ \ddot{\phi} &= \dot{\theta} \dot{\psi} \left(\frac{I_y - I_z}{I_x} \right) + \frac{L}{I_x} \tau_\phi \\ \ddot{\theta} &= \dot{\phi} \dot{\psi} \left(\frac{I_z - I_x}{I_y} \right) + \frac{L}{I_y} \tau_\theta \\ \ddot{\psi} &= \dot{\phi} \dot{\theta} \left(\frac{I_x - I_y}{I_z} \right) + \frac{1}{I_z} \tau_\psi \end{aligned} \quad (53)$$

where x, y, z represent the center of mass position in an inertial frame and ϕ, θ, ψ are the roll, pitch, and yaw angles of the quadrotor body frame, respectively, in the inertial frame [64].

m is the mass of the quadrotor; I_x, I_y, I_z are the moments of inertia. A linearized model of (53) around the hover equilibrium point is given by:

$$\begin{aligned} \ddot{x} &= g\theta & \ddot{\theta} &= \frac{L}{I_y}\tau_\theta \\ \ddot{y} &= -g\phi & \ddot{\phi} &= \frac{L}{I_x}\tau_\phi \\ \ddot{z} &= \frac{\Delta f_z}{m} & \ddot{\psi} &= \frac{1}{I_z}\tau_\psi \end{aligned} \tag{54}$$

where $\Delta f_z = f_z - mg$. We utilize (54) as a design model for the AC-RL, MSAC-RL, and HTAC-RL controllers, and (53) as the underlying simulation model for the numerical experiment. As (54) and (52) form a linear & controllable system, the representation given by (36) is admitted, and thus the adaptive control algorithms developed in the previous sections may be applied (when the linearized system is used as the design model).

The model in (53) is implemented using an RK4 integration scheme with a step of 1 millisecond. The following parameters are used to construct the reference environment: $I_x = I_y = .22kg \cdot m^2$, $I_z = .44kg \cdot m^2$, $m = 1.2kg$, $L = .30m$. The control input is updated every 50 milliseconds to emulate latencies arising from measurement, communication, actuation and computation.

3.4.2 Quadrotor Landing Task

Due to the strength of RL algorithms in solving "unconstrained" control problems, we are free to define the landing task in an elegant and concise manner (instead of having to formulate a convex/simplified objective to enable tractable solutions via LQR or MPC). We assume that a platform of known inertial position is moving with known inertial velocity. The goal is to utilize full state feedback to determine a control policy that enables a quadrotor to land on the moving platform from a wide array of initial conditions. Let Δz and Δxy be the inertial vertical distance and lateral distance, respectively, from the quadrotor to the platform. Furthermore, let $v_{xy} = \sqrt{\dot{x}^2 + \dot{y}^2}$ be the quadrotor's lateral velocity. We define the boolean variable `box` to be True if ALL of the following simultaneously hold: $|\Delta z| \leq z_{max}$; $|\Delta xy| \leq l_{max}$; $|\phi| \leq \phi_{max}$; $|\theta| \leq \theta_{max}$; $|v_{xy}| \leq v_{l,max}$; $|v_z| \leq v_{z,max}$, where $z_{max}, l_{max}, \phi_{max}, \theta_{max}, v_{l,max}, v_{z,max}$ are user provided parameters that determine if the quadcopter has successfully landed.

A ternary cost function then quite naturally defines the control objective:

$$c(\vec{x}, t) = \begin{cases} -1 & \text{box} \\ 1 & \neg \text{box} \wedge (\Delta z \leq 0 \vee t \geq T_{max}) \\ 0 & \text{else} \end{cases} \tag{55}$$

where \vec{x} captures the whole quadrotor state. The first case in (55) defines success, the second case represents failure either due to a crash or a timeout, and the third is a neutral case and therefore set to zero. This cost function is a natural formulation for the problem at hand, as the goal is to have the quadrotor land as quickly and accurately as possible. Because the function is complex and non-quadratic, standard optimal control methods become inadequate. RL is a good alternative as it allows the determination of a policy with such a cost function.

3.4.3 Reinforcement Learning

PPO [73] is used to learn an appropriate feedback policy π in order to solve the optimization problem in (17). The actor and critic networks each have two hidden layers; each layer contains 64 neurons and uses tanh activation functions. A learning rate of $1e-4$, a discount factor of .99, a clipping range of .2, and a generalized advantage estimator discount of .95 are used as hyperparameters. Applying the PPO algorithm to the reference environment with the cost function in (55) results in the successful training of a feedback policy π , which accomplishes the task when no parametric uncertainties or loss of propeller effectiveness are present.

3.4.4 Loss of Effectiveness

The trained policy is applied to a target environment with parametric uncertainties. In our tests parametric uncertainties are induced by abruptly introducing a loss of thrust effectiveness of the fourth quadrotor propeller. This can occur if the propeller blades are broken midflight, as demonstrated in [64]. This corresponds to the target-system structure as in (35), with the symmetric part of Λ^* being positive definite. For example, if the fourth propeller experienced a 50% loss of effectiveness $\Lambda^* = \text{diag}(1.0, 1.0, 1.0, 0.5)$. The AC-RL, HTAC-RL, and MSAC-RL approaches are tested with such a loss-of-effectiveness (LOE). Two success criteria are measured: success rate (SR) and success time (ST). These methods are compared to a straightforward RL approach in which the learned policy π is applied directly to the target system so as to maximize the success criteria.

AC-RL	HTAC-RL	MSAC-RL	RL	LOE
SR	SR	SR	SR	
97%	97%	97%	97%	0%
88%	90%	88%	74%	10%
75%	72%	73%	34%	25%
47%	50%	54%	14%	50%
4%	9%	27%	0%	75%
AC-RL	HTAC-RL	MSAC-RL	RL	LOE
ST	ST	ST	ST	
2.6s	2.6s	2.6s	2.6s	0%
3.1s	2.7s	3.1s	3.1s	10%
2.8s	2.6s	2.9s	4.7s	25%
3.4s	3.0s	3.3s	5.4s	50%
3.6s	3.1s	3.3s	--	75%

Table 1: Results from the simulated quadrotor experiments. The LOE column represents the degree of propeller thrust lost (with 0% being no loss). All three adaptive control methods outperform the standard RL approach in the case of non-zero LOE, across both metrics. Success time is measured as the mean time required to complete a task, averaged over all successful tests. For a 75% LOE there is no data on the RL success time because there were no successful tests. No measurement noise was introduced in these experiments.

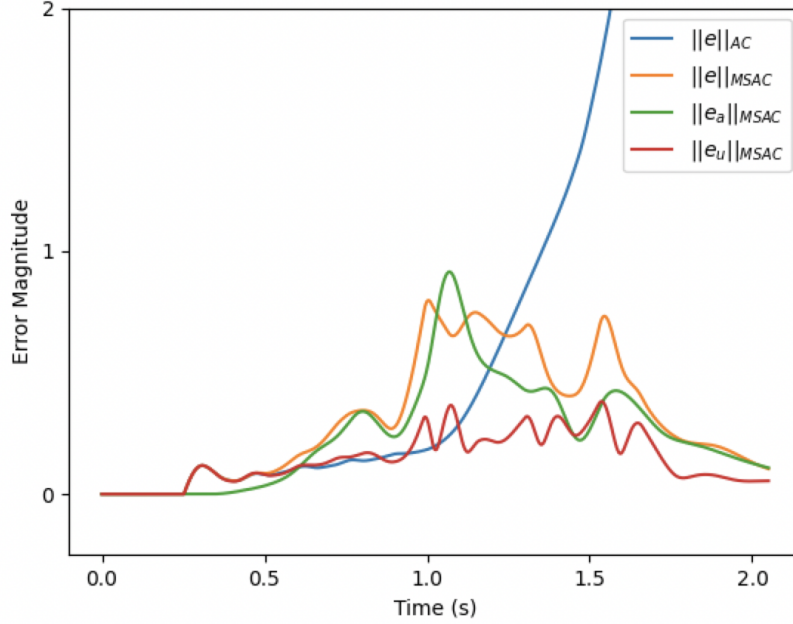


Figure 1: Comparison of error signals used by the AC-RL algorithm (blue) and those used by the MSAC-RL variant in a 60% LOE quadrotor evaluation. The AC-RL algorithm ultimately fails the task, while MSAC-RL succeeds. Because the error signals are vectors in \mathbb{R}^{12} only the vector magnitudes have been plotted.

As shown in Table 1, all three adaptive control algorithms perform better than RL, with the improvement becoming larger as the LOE increases. Furthermore, MSAC-RL and HTAC-RL improve upon AC-RL, with the former achieving better success rates at higher LOE, and the latter achieving faster completion times. Figure 1 compares the error signals involved in MSAC-RL to the error signal used in adaptive control, and shows that in the given run MSAC-RL manages to keep the error signal magnitudes low by accommodating the input-saturation which the AC-RL does not.

3.4.5 Loss of Effectiveness with Noise

We further studied (experimentally) the efficacy of AC-RL when noise is introduced into the system. A set of new reference environments are constructed, in which aleatoric measurement noise is introduced. Two reference environments are used - one with positional measurement noise only, and one with positional and orientation measurement noise. In each case the noise is taken to be zero mean and normally distributed - this may correspond, for example, to posterior position/orientation estimates that result from a Kalman filtering algorithm. RL is used to train a policy for each of these environments, and the AC-RL and RL approaches are tested on the quadrotor task with LOE and the appropriate measurement noise. The results are reported in Tables 2 and 3, which clearly indicate the large improvement of AC-RL over RL.

AC-RL SR	RL SR	LOE
91%	91%	0%
66%	38%	25%
31%	2%	50%

Table 2: Success rates for LOE with position measurement noise. Measurement of the Cartesian positions x, y, z contain additive aleatoric uncertainty given by random variables drawn from $\mathcal{N}(0, 0.05)$

AC-RL SR	RL SR	LOE
84%	84%	0%
51%	25%	25%
23%	0%	50%

Table 3: Success rates for LOE with position and orientation measurement noise. Measurement of the Cartesian positions x, y, z contain additive aleatoric uncertainty given by random variables drawn from $\mathcal{N}(0, 0.05)$ and ϕ, θ, ψ are perturbed by random variables drawn from $\mathcal{N}(0, 5\frac{\pi}{365})$.

3.5 Extensions

The class of problems for which the three algorithms proposed above result in stability and constant Regret is given by (35), with the corresponding Lyapunov function chosen to be quadratic as in (94). Several extensions to this class are possible, one of which is control-affine systems [59]

$$\dot{x} = A(x) + B(x)(u + \Phi(x)\theta)$$

where $A(\cdot), B(\cdot), \Phi(\cdot)$ are nonlinear functions of their arguments, by allowing the Lyapunov functions to be nonquadratic that leverage the nonlinear forms of $A(\cdot)$ and $B(\cdot)$. Yet another extension corresponds to nonlinear systems that are not feedback linearizable, with triangular structures as in [5], by combining the control structures proposed here with suitable backstepping components. These extensions are not addressed here simply due to space limitations. Finally, the control structures of AC-RL, HTAC-RL, and MSAC-RL were predicated on the assumption that the state was fully accessible. Extensions to the case of partial state feedback remain to be carried out using AC methods with output feedback and RL approaches based on partially observable MDP, which are topics for future research. Stochastic counterparts of all of the treatment above can be carried using analytical tools from the stochastic adaptive control literature, which is a topic for future research as well.

4 Online Estimation Policies - Discrete Time

We now focus on the problem of estimation of outputs and parameters in a discrete-time dynamic system in the presence of parametric uncertainties and noise. We address the problem of accelerated performance, i.e. fast output estimation, and problem of accelerated learning, i.e. fast parameter convergence. The solutions proposed are a set of online algorithms devel-

oped using a combination of adaptive and ML approaches. Numerical validation is carried out using benchmark problems in ML.

4.1 A High Order Tuner for Accelerated Performance

Instead of a gradient-based update as in (30), our goal is to derive a second-order tuner that is Nesterov-type and includes terms that incorporate momentum and acceleration. For this purpose, we consider the objective function in (34). Following an update in the parameter as in (30), we note that both estimator in (26) and the output error in (27) can be updated as well, leading to a-priori and a-posteriori errors

$$e_{y,k} = \phi_{k-1}^T \theta_{k-1} - \phi_{k-1}^T \theta^* - \eta_k \quad (56)$$

$$e_{y,k}^{ap} = \phi_{k-1}^T \theta_k - \phi_{k-1}^T \theta^* - \eta_k \quad (57)$$

which in turn leads to the gradients as in (29) and an a-posteriori gradient

$$\nabla_{\theta_k} \left(\frac{1}{2} (e_{y,k}^{ap})^2 \right) = \phi_{k-1} \left(\phi_{k-1}^T \theta_k - \phi_{k-1}^T \theta^* - \eta_k \right) \quad (58)$$

With a slight abuse of notation, we will denote this a-posteriori gradient as $\nabla_{\theta_k} L_k$.

This in turn leads to an a-priori gradient for f_k as

$$\nabla f_k(\theta_{k-1}) = \frac{\nabla_{\theta_{k-1}} L_k}{\mathcal{N}_{k-1}} + \mu(\theta_{k-1} - \theta_0) \quad (59)$$

and an a-posteriori gradient

$$\nabla f_k(\theta_k) = \frac{\nabla_{\theta_k} L_k}{\mathcal{N}_{k-1}} + \mu(\theta_k - \theta_0) \quad (60)$$

We now propose the high-order tuner (HT):

$$\vartheta_k = \vartheta_{k-1} - \gamma \nabla f_k(\theta_k), \quad (61)$$

$$\bar{\theta}_{k-1} = \theta_{k-1} - \gamma \beta \nabla f_k(\theta_{k-1}), \quad (62)$$

$$\theta_k = \bar{\theta}_{k-1} - \beta(\bar{\theta}_{k-1} - \vartheta_{k-1}). \quad (63)$$

That is, the update from θ_{k-1} to θ_k occurs using a second-order tuner as in (61)-(63), that includes both acceleration based momentum based components. The use of the a-posteriori gradient in (61) provides an acceleration component similar to that in Nesterov's algorithm in (32) while the rotation of the update as in (62) can be viewed as a momentum term. It should be noted however that the presence of the time-varying regressor ϕ_k in the overall problem causes this HT to be fundamentally different from Nesterov's algorithm in (32). This difference is key to establishing its stability, which cannot be ensured in Nesterov's algorithm when the regressor ϕ_k varies with k . In what follows, we first present the results when there is no noise, and then present the noisy case.

4.1.1 Noise-free case

We now present the key stability and convergence results for the HT when $\eta_k \equiv 0$ in (24).

Theorem 4. For the linear regression error model in (27) with loss in (28), the HT in (61)-(63) with its hyperparameters chosen as $\mu = 0$, $0 < \beta < 1$, and $0 < \gamma \leq \frac{\beta(2-\beta)}{16+\beta^2}$ leads to the following Lyapunov function

$$V_k = \frac{1}{\gamma} \|\vartheta_k - \theta^*\|^2 + \frac{1}{\gamma} \|\theta_k - \vartheta_k\|^2, \quad (64)$$

with $\Delta V_k \leq -\frac{L_k}{N_{k-1}} \leq 0$. In addition to $V \in \ell_\infty$, it can be shown that $\lim_{k \rightarrow \infty} L_k = 0$.

In addition to the above stability properties, the HT has another attractive property, of accelerated convergence rate when the regressors are constant and no noise is present. Before stating the theorem, we establish the equivalence between the HT in (61)-(63) and Nesterov's equations in (32) in the following proposition. The reader is referred to [50] for its proof.

Proposition 1. If $\phi_k \equiv \phi$, where ϕ is a constant vector, defining constants $\bar{\beta} = 1 - \beta$ and $\bar{\alpha} = \gamma\beta$, Eqs. (61)-(63) can be transformed as

$$\begin{aligned} \theta_k &= \nu_{k-1} - \bar{\alpha} \nabla f(\nu_{k-1}), \\ \nu_k &= (1 + \bar{\beta})\theta_k - \bar{\beta}\theta_{k-1}, \end{aligned} \quad (65)$$

which coincides with Eq. 2.2.22 in [56].

With the above equivalence established, we now state the acceleration property of the HT in Theorem 5. The reader is referred to [21, 74] for its proof. The following choice of hyperparameters in (65) is made:

$$\begin{aligned} \theta_0 &= \nu_0 & \mu &= \epsilon/\Psi & \bar{L} &= 1 + \mu \\ \bar{\alpha} &= 1/\bar{L} & \kappa &= \bar{L}/\mu & \bar{\beta} &= (\sqrt{\kappa} - 1)/(\sqrt{\kappa} + 1) \end{aligned} \quad (66)$$

where $\Psi \geq \max\{1, \|\theta_0 - \theta^*\|^2\}$ for unnormalized loss functions and $\Psi \geq \max\{1, \mathcal{N}\|\theta_0 - \theta^*\|^2\}$ for normalized loss functions.

Theorem 5. For a \bar{L} -smooth and μ -strongly convex function f , the iterates $\{\theta_k\}_{k=0}^\infty$ generated by (65) with hyperparameters as in (66) satisfy

$$f(\theta_k) - f(\theta^*) \leq \frac{\bar{L} + \mu}{2} \|\theta_0 - \theta^*\|^2 \exp\left(-\frac{k}{\sqrt{\kappa}}\right).$$

Theorem 5 establishes the acceleration properties for the regularized loss function in (34). This is in turn utilized to establish the acceleration properties for both the normalized and unnormalized loss functions, summarized below in Lemmas 1 and 2.

Lemma 1. With the hyperparameters of (65) chosen as in (66), it follows that

$$\frac{L(\theta_k) - L(\theta^*)}{\mathcal{N}} \leq \epsilon, \text{ if } k \geq \left\lceil \sqrt{1 + \frac{\Psi}{\epsilon}} \log\left(2 + \frac{\Psi}{\epsilon}\right) \right\rceil. \quad (67)$$

Lemma 2. With the hyperparameters of (65) chosen as in (66), it follows that

$$L(\theta_k) - L(\theta^*) \leq \epsilon, \text{ if } k \geq \left\lceil \sqrt{1 + \frac{\Psi}{\epsilon}} \log\left(2 + \frac{\Psi}{\epsilon}\right) \right\rceil. \quad (68)$$

Remark 5. The inequalities (67) and (68) show that a lower bound can be derived on the number of iterations needed to get convergence. They show that an ϵ -optimal convergence can be guaranteed using an $\mathcal{O}(1/\sqrt{\epsilon} \cdot \log(1/\epsilon))$ with the HT in (61)-(63) both for the unnormalized and the normalized loss functions.

Remark 6. It can be noted from both Lemmas 1 and 2 that the L2 regularization parameter μ in (34) is smaller than the ϵ sub-optimality gap. The L2 regularization parameter is present to ensure strong convexity of the augmented objective function in (34). This in turn enabled the reduction of the HT to Nesterov's iterative method with constant gains as in (65).

4.1.2 Stability properties of the HT in the presence of noise

In this case, the starting point is the regression model in (24) with $\eta_k \neq 0$.

Theorem 6. For the stochastic linear regression model in (56) and (57), if noise assumptions (22)-(23) are satisfied, the adaptive law in (61)-(63) with $0 < \mu < 1$, $0 < \beta < 1$, $0 < \gamma \leq \frac{\beta(2-\beta)}{16+\beta^2+\mu\left(\frac{57\beta+1}{16\beta}\right)}$ results in the sequence $V(x_k)$ converging exponentially fast to a compact set defined as $M = \{V|V \leq K\}$, where $K = \max\left\{\frac{c_2^2}{(\alpha-c_1)^2}, \frac{\hat{c}}{\alpha}\right\}$, at a rate no slower than $1 - \alpha$, for any $0 < \alpha < c_1$.

4.1.3 Numerical Validation of the High Order Tuners

We first illustrate the stability property of HT in Theorem 4 and the convergence property in Lemma 1. For this purpose, we choose an L_k of the form [21, P. 69]

$$L_k(\theta) = \frac{a_k}{4} \left\{ \frac{1}{2} \left[b_k(\theta^{(1)})^2 + c_k \sum_{i=1}^{n-1} (\theta^{(i)} - \theta^{(i+1)})^2 + b_k(\theta^{(n)})^2 \right] - d_k \theta^{(1)} \right\}, \quad (69)$$

where a_k, b_k, c_k and d_k are positive scalars which depend on the iteration k , and the superscript (i) indicates the i -th element of the vector θ .

It can be shown that L_k is a quadratic non-homogeneous function of θ , and admits a unique minimum of the form [21, P. 69]

$$\theta_k^{*(i)} = d_k \left[\frac{(n-i)b_k + c_k}{(n-1)b_k^2 + 2b_k c_k} \right] \text{ for } 1 \leq i \leq n, \quad (70)$$

which does not depend on a_k . It is also noted that the gradient and Hessian are given by

$$\nabla L_k(\theta) = 2\phi_k \phi_k^T \theta + B_k, \quad (71)$$

where

$$B_k = -\frac{a_k}{4} [d_k, 0, \dots, 0]^T \quad (72)$$

and

$$\nabla^2 L_k(\theta) = 2\phi_k \phi_k^T \leq \bar{L}I, \quad (73)$$

where

$$\phi_k^T = \frac{\sqrt{2a_k}}{4} \begin{bmatrix} \sqrt{b_k} & 0 & \cdots & 0 & 0 & 0 \\ 0 & 0 & \cdots & 0 & 0 & \sqrt{b_k} \\ \sqrt{c_k} & -\sqrt{c_k} & \cdots & 0 & 0 & 0 \\ \vdots & \vdots & \ddots & \vdots & \vdots & \vdots \\ 0 & 0 & \cdots & \sqrt{c_k} & -\sqrt{c_k} & 0 \\ 0 & 0 & \cdots & 0 & \sqrt{c_k} & -\sqrt{c_k} \end{bmatrix} \quad (74)$$

In what follows, we assume $n = 400$, $b_k = c_k = d_k = 1$ unless otherwise specified, and allow the L -smoothness parameter to vary by changing a_k . The results for three different cases of these variations are shown in Figure 2 where the HT is compared with several other algorithms, showing the significant advantage of the proposed HT.

4.1.4 Extension to Convex Functions

Unlike the previous example, where the underlying Loss function is quadratic in the parameters as in (28), we now consider a general loss function that is convex in θ_k , i.e.,

$$\min_{\theta \in \mathbb{R}^N} L_k(\theta). \quad (75)$$

We propose a recursive high-order tuner to find θ , similar to equations (61)-(63), but with the following two distinctions:

- The choice of the normalizing signal \mathcal{N}_k :

$$\mathcal{N}_k = 1 + H_k, \quad (76)$$

where H_k is defined as

$$H_k = \max \left\{ \lambda : \lambda \in \sigma(\nabla^2 L_k(\theta)) \right\}, \quad (77)$$

and $\sigma(\nabla^2 L_k(\theta))$ denotes the spectrum of the Hessian matrix of the loss function L_k .

- Instead of the augmented function f in (34), we choose a normalized loss function $\bar{f} = \frac{L_k(\theta_k)}{\mathcal{N}_k}$. This high-order tuner is summarized in equations (78)-(80).

$$\vartheta_k = \vartheta_{k-1} - \gamma \nabla \bar{f}_k(\theta_k), \quad (78)$$

$$\bar{\theta}_{k-1} = \theta_{k-1} - \gamma \beta \nabla \bar{f}_k(\theta_{k-1}), \quad (79)$$

$$\theta_k = \bar{\theta}_{k-1} - \beta(\bar{\theta}_{k-1} - \vartheta_{k-1}). \quad (80)$$

Equations (78)-(80) implies that at each k , in addition to the first moment, ∇L_k , we also have access to the second moment, H_k , as well, in the form of (77). In many engineering problems, the underlying model includes prior information regarding the causality of the loss function [75]. Both the first and second moment may be functions of the regressor, with $\nabla L_k = g(\phi_k)$, and $H_k = h(\phi_k)$, where ϕ_k is the value of the regressor during iteration k . The prior information may then imply that $g(\cdot)$ and $h(\cdot)$ are known functions, allowing Algorithm 2 to be implemented at each k . If these functions are poorly known, then conservative choices

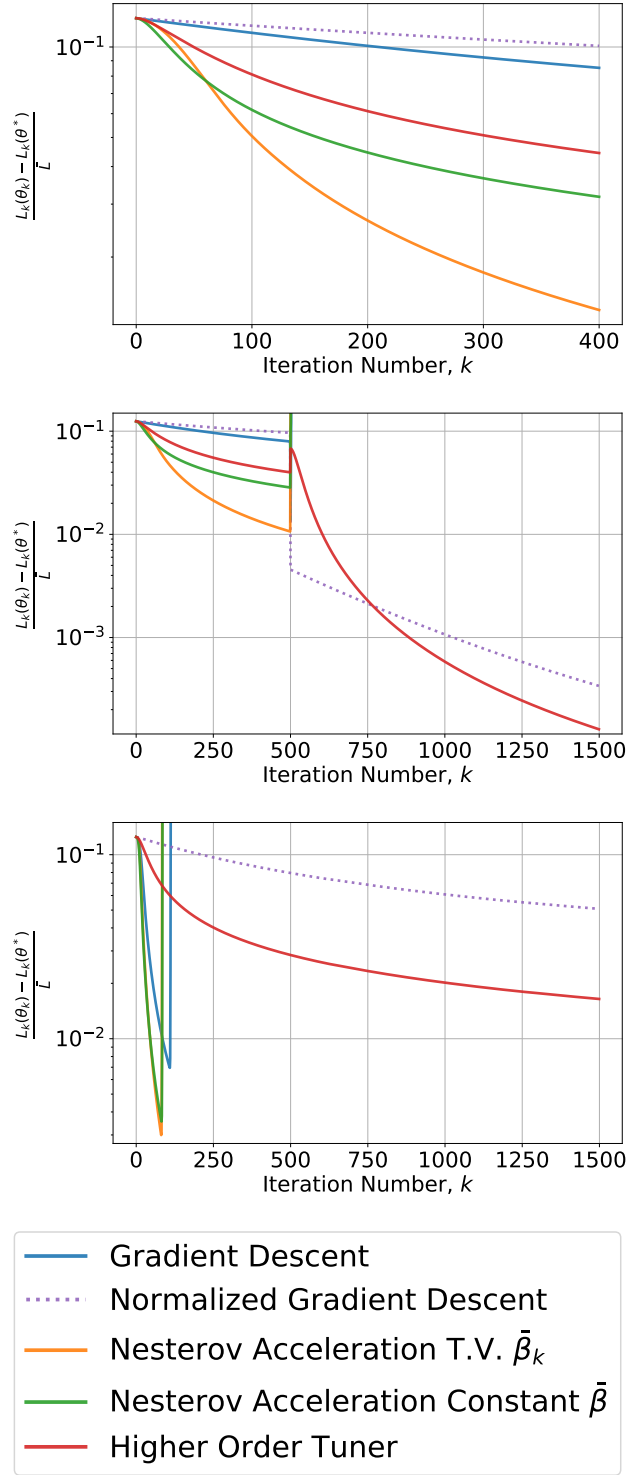


Figure 2: Smooth convex minimization hyperparameters chosen as $\mu = 10^{-5}$, $\beta = 0.1$ and $\gamma = 0.01186$. First figure: $a_k = 2$; Second figure: $a_k = 2$, b_k and c_k changed to 2000 and 1500, respectively, at $k = 500$; Third figure: $a_k = 8000$; Fourth figure: Legend.

have to be made in the implementations of ∇L_k and H_k . For example, the second moment can be chosen as $H_k = \bar{L}$ where \bar{L} is the smoothness parameter of L_k .

The following two theorems summarize the underlying stability and convergence properties of the HT optimizer. The reader is referred to further details and proofs of these theorems to [49, 52].

Theorem 7. *For a continuously differentiable \bar{L}_k -smooth convex loss function $L_k(\cdot)$, equations (78)-(80), with $0 < \beta < 1$ and $0 < \gamma \leq \frac{\beta(2-\beta)}{8+\beta}$, ensures that $V = \frac{1}{\gamma}\|\vartheta - \theta^*\|^2 + \frac{1}{\gamma}\|\theta - \vartheta\|^2$ is a Lyapunov function. It can also be shown that $V \in \ell_\infty$, and $\lim_{k \rightarrow \infty} L_k(\theta_{k+1}) - L_k(\theta^*) = 0$.*

Theorem 8. *For a continuously differentiable \bar{L}_k -smooth and μ -strongly convex loss function $L_k(\cdot)$, equations (78)-(80), with $0 < \beta < 1$ and $0 < \gamma \leq \frac{\beta(2-\beta)}{16+\beta+\mu}$ ensures that $V = \frac{1}{\gamma}\|\vartheta - \theta^*\|^2 + \frac{1}{\gamma}\|\theta - \vartheta\|^2$ is a Lyapunov function. It can also be shown that $V \in \ell_\infty$, and $\lim_{k \rightarrow \infty} L_k(\theta_{k+1}) - L_k(\theta^*) = 0$. Furthermore, for constant regressors (i.e.: $\mathcal{N}_k = \mathcal{N}$), $V_k \leq \exp(-\mu C k)V_0$, where $C = \frac{\gamma\beta}{4N}$.*

4.2 An Algorithm with Time-varying Learning Rate for Accelerated Learning

We now return to the regression model in (24), with its estimation as in (26). The problem of interest here is to have an accelerated learning of the parameter in terms of fast convergence of θ_k to θ^* . For ease of exposition, only the noise-free case is considered. We propose the following new recursive algorithm (TVLR) for estimating θ^* as θ_k , for all $k \geq 0$:

$$\theta_{k+1} = \theta_k - \frac{\lambda_\Gamma \kappa \Gamma_k \phi_k e_k}{1 + \|\phi_k\|^2}, \quad (81)$$

$$\Omega_k = (1 - \lambda_\Omega) \Omega_{k-1} + \frac{\phi_k \phi_k^T}{1 + \|\phi_k\|^2}, \quad (82)$$

$$\Gamma_k = \Gamma_{k-1} + \lambda_\Gamma (\Gamma_{k-1} - \kappa \Gamma_{k-1} \Omega_k \Gamma_{k-1}), \quad (83)$$

where λ_Γ , κ are positive scalars and $\Gamma_k \in \mathbb{R}^{N \times N}$ is the time-varying gain matrix. The initial value Γ_0 is a symmetric positive definite matrix chosen so that $\Gamma_0 \preceq \Gamma_{\max} I$, where $\Gamma_{\max} \in \mathbb{R}^+$ is the maximum learning rate that is assumed to be given. The information matrix $\Omega_k \in \mathbb{R}^{N \times N}$ captures any excitation that may be present in the regressor ϕ_k . The initial value of Ω_k is a symmetric positive definite matrix with $0 \prec \Omega_0 \preceq I$. The parameter $0 < \lambda_\Omega < 1$ is used for the adjustment of the evolution of Ω_k and is directly related to the upper bound of Ω_k . The scalars λ_Γ , κ and λ_Ω represent various weights of the proposed algorithm.

The main innovation in the algorithm above is in the evolution of Γ_k . Unlike the recursive least squares algorithm (see [19] for example) with covariance resetting introduced via an externally chosen period, the algorithm in (83) automatically ensures that Γ_k stays within certain bounds, through a combination of linear and nonlinear components. As will be shown in the following section, stability and exponential decrease of parameter error towards a compact set are established with persistent excitation. When PE conditions are not satisfied, addition of a suitable projection can ensure stable estimation [76], details of which are not addressed in this paper.

We first establish a lower bound of Ω_k under conditions of persistent excitation in Lemma 3. We then use this lower bound to show the boundedness of the time-varying learning rate

Γ_k in Lemma 4. The proof of Lemma 3 is straightforward and therefore omitted. The proof of Lemma 4 is included in the Appendix.

Lemma 3. *If $0 < \lambda_\Omega < 1$, and ϕ_k is persistently exciting over a period ΔT at a level α for all $k \geq k_1$, then $\Omega_k \succeq \Omega_{PE}I$, $\forall k \geq k_2$, where $\Omega_{PE} = (1 - \lambda_\Omega)^{\Delta T - 1}\alpha$ and $k_2 = k_1 + \Delta T$.*

Lemma 4. *If ϕ_k is persistently exciting, $\Omega_{PE}I \preceq \Omega_k \preceq \Omega_{\max}I$, $\forall k \geq k_2$, learning rate gain $0 < \lambda_\Gamma < \min \left\{ \frac{1}{\Omega_{\max}/\Omega_{PE} - 1}, 1 \right\}$, gain $\kappa_{\min} \leq \kappa < \kappa_{\max}$, and initial value $\Gamma_{PE}I \preceq \Gamma_{k_2} \preceq \Gamma_{\max}I$, then $\Gamma_{PE}I \preceq \Gamma_k \preceq \Gamma_{\max}I$, $\forall k > k_2$ for some $k_2 > k_1$.*

We now show that with these bounded time-varying learning rates, the parameter estimate θ_k will remain bounded and that it will converge to θ^* . For this purpose, we choose the parameters in (81)-(83) as follows:

$$\lambda_\Omega > \frac{1}{\Omega_{PE} + 1}, \quad (84)$$

$$0 < \lambda_\Gamma < \min \left\{ \frac{1}{\Omega_{\max}/\Omega_{PE} - 1}, 1, \Omega_{PE} \right\}. \quad (85)$$

We define

$$\kappa_{\min} = \frac{1}{\Gamma_{\max}\Omega_{PE}}, \quad (86)$$

$$\kappa_{\max} = \min \left\{ \frac{1 + \lambda_\Gamma}{\lambda_\Gamma\Omega_{\max}\Gamma_{\max}}, \frac{1}{\lambda_\Gamma\Gamma_{\max}}, \frac{1}{(1 - \lambda_\Omega)\Omega_{\max}\Gamma_{\max}} \right\} \quad (87)$$

and choose any κ that satisfies

$$\kappa_{\min} \leq \kappa < \kappa_{\max}. \quad (88)$$

Define a matrix

$$\bar{\Gamma}_k = \Gamma_{k-1} - \lambda_\Gamma\kappa\Gamma_{k-1} \frac{\phi_{k-1}\phi_{k-1}^T}{1 + \|\phi_{k-1}\|^2} \Gamma_{k-1}, \quad (89)$$

and consider a Lyapunov function candidate

$$V_k = \tilde{\theta}_k^T \bar{\Gamma}_k^{-1} \tilde{\theta}_k. \quad (90)$$

Theorem 9. *Let ϕ_k be persistently exciting. For the model and estimator given by (24) and (26), the algorithm in (81)-(83) with the constants chosen as in (84)-(88) guarantees that*

$$V_k \leq \exp[-\mu_2(k - k_2)] V_{k_2}, \quad \forall k \geq k_2$$

4.2.1 Numerical validation of the algorithm with time-varying learning rate

We demonstrate the stability of the TVLR algorithm by considering the same loss function in (69). In order to account for the nonhomogeneous feature of the loss function, the update in θ_k was modified to include ∇L_k rather than $\phi_k e_k$. In addition to the gradient descent algorithm and normalized gradient descent algorithm, we also compared the TVLR algorithm with the well-known AdaGrad [77], which can be considered as a robust version of the stochastic gradient descent with time-varying learning rates. The results in Figure 3 show that the TVLR algorithm is comparable to AdaGrad in terms of convergence performance. More importantly, our algorithm does not exhibit the unstable behavior near the smoothness step change around iteration 500 exhibited by AdaGrad.

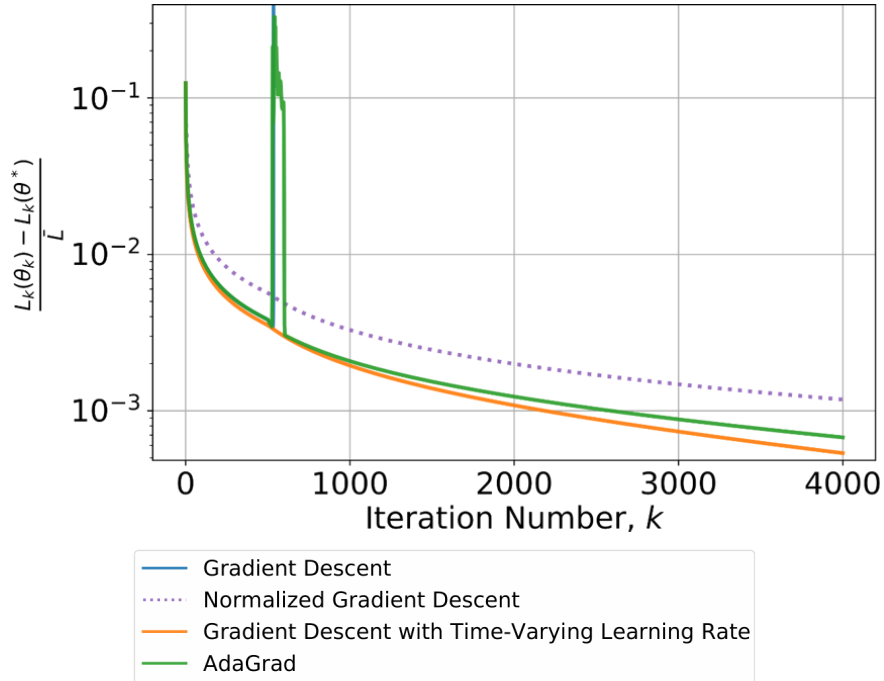


Figure 3: Minimization of the loss in Equation (69). The hyperparameters are chosen as follows: a_k changes from 2 to 8 at iteration number 500.

4.3 Observations and Extensions

We presented two algorithms for estimation in discrete-time in Sections 4.1 and 4.2, with the focus of the first on accelerated performance, i.e. fast convergence of the loss function L_k to zero, and that of the second on fast learning, i.e. convergence of the parameter estimate $\hat{\theta}_k$ to its true value θ^* . Numerical validation is carried out using benchmark problems in ML. The first algorithm is a high-order tuner, a discrete-time version of the algorithm in (43), and is shown to be stable with time-varying regressors, advantageous when compared with Nesterov’s algorithm, ensures accelerated performance, and extendable to general convex functions. The second algorithm includes time-varying learning rates and is shown to lead to exponential convergence of the parameter estimate to its true value with persistent excitation. What remains to be seen is if a combination of these two algorithms can simultaneously exhibit accelerated performance and accelerated learning, a topic for future research.

5 Summary and Conclusions

This paper proposed solutions for real time control and learning in dynamic systems using a combination of adaptive and machine learning approaches. The first class of solutions focused on continuous time systems and combines adaptive control with reinforcement learning, with provable guarantees and significant improvement in numerical validation of a challenging online control task. Three different algorithms, AC-RL, HTAC-RL, and MSAC-RL were presented, with HTAC-RL providing an improvement over the first in terms of accelerated performance, and MSAC-RL providing yet another improvement, in terms of accommodating input-constraints. In all cases, the focus was on real-time control, analytical

guarantees of global boundedness, and constant Regret. The second class of solutions focused on discrete-time systems and combines adaptive algorithms with machine learning methods with emphasis on accelerated performance. Some of the algorithms proposed are shown to result in stability with time-varying regressors unlike their ML counterparts while retaining the accelerated performance properties; others are shown to result in accelerated parameter learning, once again with provable guarantees and demonstrable improvement in numerical experiments. Together, this paper takes a first step towards online machine learning with provable guarantees by drawing upon key insights, tools, and approaches developed in these two disparate and powerful methodologies of adaptive control and estimation and machine learning. Several more steps need to be carried out in this direction and address extensions to more complex nonlinear systems with nonconvex costs leading to more optimal performance.

6 Appendix

Key steps in the proofs of all theorems and lemmas above are given below. A more detailed proof for Theorem 6 can be found in [51].

As Theorems 1-3 pertain to the same plant (35), reference system (36), and control input in (8), the following derivation is common to their proofs. From Assumption A3 and Eq. (7), it follows that a K^* exists such that

$$B_r \Lambda^* K^* = B_r \quad (91)$$

Using (35)-(41) and (91), we obtain the error dynamics

$$\dot{e} = A_H e + B_r \Lambda^* \tilde{\Theta} \omega, \quad (92)$$

where $\tilde{K} = K - K^*$, $\tilde{\Theta}_l = \Theta_l - \Theta_l^*$ and $\tilde{\Theta}_{nl} = \Theta_{nl} - \Theta_{nl}^*$, $\tilde{\Theta} = [\tilde{K}, \tilde{\Theta}_{nl}, \tilde{\Theta}_l]$ and $\omega = [u_{\text{exog}}^T, -\phi^T(x), x^T]^T$.

6.1 Proof of Theorem 1:

Proof. The adaptive laws in (39)-(41) can be compactly written as

$$\dot{\tilde{\Theta}} = -\Gamma B_r^T P e \omega^T. \quad (93)$$

where Γ is a block-diagonal matrix with its entries as Γ_K , $\Gamma_{\Theta_{nl}}$, and Γ_{Θ_l} . The standard form of (92) leads to the Lyapunov function candidate

$$V(e, \tilde{\Theta}) = e^T P e + \text{Tr} \left(\tilde{\Theta}^T \left(\Lambda^{*T} S \right) \tilde{\Theta} \right) \quad (94)$$

where $S = \Gamma^{-1}$ in (7) with the symmetric part of $\Lambda^* S$ positive-definite. Using arguments as in [78], we can show that $\dot{V} = -e^T Q e$ by using the update laws as (39)-(41). Thus, $e(t)$ and the parameter estimates K, Θ_{nl}, Θ_l are uniformly bounded. This, along with Assumption A4', implies that $\dot{e}(t)$ is bounded. It follows from Barbalat's lemma that $\lim_{t \rightarrow \infty} \|e(t)\| = 0$. \square

6.2 Proof of Theorem 2:

Proof. We start with the error dynamics (92). Consider the following candidate Lyapunov function

$$\begin{aligned} V = & \frac{1}{\gamma} \text{Tr} \left[(\Xi - \Theta^*)^T \Lambda^{*T} (\Xi - \Theta^*) \right] \\ & + \frac{1}{\gamma} \text{Tr} \left[(\Theta - \Xi)^T \Lambda^{*T} (\Theta - \Xi) \right] + e^T P e \end{aligned} \quad (95)$$

Using (42), (43), (44) and (92), the time derivative of (95) can be shown to satisfy

$$\begin{aligned} \dot{V} = & \frac{1}{\gamma} \text{Tr} \left[\dot{\Xi}^T \Lambda^{*T} (\Xi - \Theta^*) + (\Xi - \Theta^*)^T \Lambda^{*T} \dot{\Xi} \right] \\ & + \frac{1}{\gamma} \text{Tr} \left[(\dot{\Theta} - \dot{\Xi})^T \Lambda^{*T} (\Theta - \Xi) + (\Theta - \Xi)^T \Lambda^{*T} (\dot{\Theta} - \dot{\Xi}) \right] \\ & + (A_H e + B_r \Lambda^* \tilde{\Theta} \omega)^T P e + e^T P (A_H e + B_r \Lambda^* \tilde{\Theta} \omega) \\ = & - \text{Tr} \left[(\Xi - \Theta^*)^T (\Lambda^* + \Lambda^{*T}) B_r^T P e \omega^T \right] \\ & - \frac{\beta}{\gamma} \text{Tr} \left[(\Theta - \Xi)^T (\Lambda^* + \Lambda^{*T}) (\Theta - \Xi) \right] \mathcal{N}_t \\ & + \text{Tr} \left[(\Theta - \Xi)^T (\Lambda^* + \Lambda^{*T}) B_r^T P e \omega^T \right] \\ & + e^T \left(A_H^T P + P A_H \right) e + 2e^T P B_r \Lambda^* \tilde{\Theta} \omega \\ = & - \frac{\beta}{\gamma} \text{Tr} \left[(\Theta - \Xi)^T (\Lambda^* + \Lambda^{*T}) (\Theta - \Xi) \right] \\ & - \frac{2\mu\beta}{\gamma} \text{Tr} \left[(\Theta - \Xi)^T (\Lambda^* + \Lambda^{*T}) (\Theta - \Xi) \right] \|\omega\|^2 \\ & - e^T Q e + 4e^T P B_r \Lambda^* (\Theta - \Xi) \omega \\ \leq & - \frac{\beta}{\gamma} \text{Tr} \left[(\Theta - \Xi)^T (\Lambda^* + \Lambda^{*T}) (\Theta - \Xi) \right] - \|e\|^2 \\ & - 4 \|P B_r\|_2^2 \text{Tr} \left[(\Theta - \Xi)^T \Omega^T \Omega (\Theta - \Xi) \right] \|\omega\|^2 \\ & + 4 \|e\| \|P B_r \Lambda^* (\Theta - \Xi)\|_F \|\omega\| \\ \leq & - \frac{\beta}{\gamma} \left\| (\Theta - \Xi)^T \Omega \right\|_F^2 - \|e\|^2 \\ & - 4 \|P B_r\|_2^2 \|(\Theta - \Xi)^T \Omega\|_F^2 \|\omega\|^2 \\ & + 4 \|\omega\| \|e\| \|P B_r\|_2 \|\Omega\|_2 \|(\Theta - \Xi)^T \Omega\|_F \\ \leq & - \frac{\beta}{\gamma} \left\| (\Theta - \Xi)^T \Omega \right\|_F^2 - \|e\|^2 \\ & - 4 \|P B_r\|_2^2 \|(\Theta - \Xi)^T \Omega\|_F^2 \|\omega\|^2 \\ & + 4 \|\omega\| \|e\| \|P B_r\|_2 \|(\Theta - \Xi)^T \Omega\|_F \\ = & - \frac{\beta}{\gamma} \left\| (\Theta - \Xi)^T \Omega \right\|_F^2 \\ & - \left[\|e\| - 2 \|P B_r\|_2 \|(\Theta - \Xi)^T \Omega\|_F \|\omega\| \right]^2 \leq 0 \end{aligned}$$

where $\|\cdot\|_F$ is the Frobenius matrix norm and $\|\cdot\|_2$ is the matrix 2-norm. In the above derivation we have used (44),(45), Assumption A5 and the inequality $\|AB\|_F \leq \|A\|_2\|B\|_F$. It can be concluded that $e, \Theta, \Xi \in \mathcal{L}_\infty$. Using Barbalat's lemma, as before, we conclude that $\lim_{t \rightarrow \infty} e(t) = 0$ and that $\mathcal{R} = O(1)$. \square

6.3 Proof of Theorem 3

Proof. With $S = \Gamma^{-1}$, we choose V as

$$V = e_u^T P e_u + \text{Tr} \left(\tilde{\Theta}^T (\Lambda^{*T} S) \tilde{\Theta} \right) + \text{Tr} \left(\tilde{K}_a^T \tilde{K}_a \right)$$

From (50) and (51), we obtain that $\dot{V} = -e_u^T Q e_u$ which allows us to conclude that $e_u, \tilde{\Theta}, \tilde{K}_a \in \mathcal{L}_\infty$. For case (i), since all parameters are bounded, a bounded input implies that the state x is bounded. Therefore $e_u \in \mathcal{L}_\infty$. Proceeding in a similar fashion to the proof of Theorem 1, Barbalat's lemma is applied to find that $\lim_{t \rightarrow \infty} \|e_u(t)\| = 0$. It is easy to show then that $\|e(t)\| = O[\int_0^t \|\Delta u(\tau)\| d\tau]$.

For case (ii), as the structure of the error model in (50) is identical to that considered in Theorem 1 in [79], the same arguments therein can be used to establish boundedness of the state. \square

6.4 Proof of Theorem 4

Proof. Consider the candidate Lyapunov function stated as

$$V_k = \frac{1}{\gamma} \|\vartheta_k - \theta^*\|^2 + \frac{1}{\gamma} \|\theta_k - \vartheta_k\|^2. \quad (96)$$

The increment $\Delta V_k := V_k - V_{k-1}$ may then be expanded using (27), (28), and equations (61)-(63) with k replaced by $k+1$ as

$$\begin{aligned} \Delta V_k &= \frac{1}{\gamma} \|\vartheta_{k+1} - \theta^*\|^2 + \frac{1}{\gamma} \|\theta_{k+1} - \vartheta_{k+1}\|^2 - \frac{1}{\gamma} \|\vartheta_k - \theta^*\|^2 - \frac{1}{\gamma} \|\theta_k - \vartheta_k\|^2 \\ \Delta V_k &= \frac{1}{\gamma} \|(\vartheta_k - \theta^*) - \frac{\gamma}{\mathcal{N}_k} \nabla L_k(\theta_{k+1})\|^2 - \frac{1}{\gamma} \|\vartheta_k - \theta^*\|^2 \\ &\quad + \frac{1}{\gamma} \|\bar{\theta}_k - \beta(\bar{\theta}_k - \vartheta_k) - \vartheta_k + \frac{\gamma}{\mathcal{N}_k} \nabla L_k(\theta_{k+1})\|^2 - \frac{1}{\gamma} \|\theta_k - \vartheta_k\|^2 \\ \Delta V_k &= \frac{\gamma}{\mathcal{N}_k^2} \|\nabla L_k(\theta_{k+1})\|^2 - \frac{2}{\mathcal{N}_k} (\vartheta_k - \theta^*)^T \nabla L_k(\theta_{k+1}) \\ &\quad + \frac{1}{\gamma} \|\bar{\theta}_k - \vartheta_k\|^2 - \frac{1}{\gamma} \|\theta_k - \vartheta_k\|^2 - \frac{\beta(2-\beta)}{\gamma} \|\bar{\theta}_k - \vartheta_k\|^2 \\ &\quad + \frac{2}{\mathcal{N}_k} (1-\beta) (\bar{\theta}_k - \vartheta_k)^T \nabla L_k(\theta_{k+1}) + \frac{\gamma}{\mathcal{N}_k^2} \|\nabla L_k(\theta_{k+1})\|^2 \\ \Delta V_k &= \frac{2\gamma}{\mathcal{N}_k^2} \|\nabla L_k(\theta_{k+1})\|^2 - \frac{2}{\mathcal{N}_k} (\theta_{k+1} - \theta^*)^T \nabla L_k(\theta_{k+1}) \\ &\quad + \frac{1}{\gamma} \|\bar{\theta}_k - \vartheta_k\|^2 - \frac{1}{\gamma} \|\theta_k - \vartheta_k\|^2 - \frac{\beta(2-\beta)}{\gamma} \|\bar{\theta}_k - \vartheta_k\|^2 \\ &\quad + \frac{2}{\mathcal{N}_k} (1-\beta) (\bar{\theta}_k - \vartheta_k)^T \nabla L_k(\theta_{k+1}) - \frac{2}{\mathcal{N}_k} (\vartheta_k - \theta_{k+1})^T \nabla L_k(\theta_{k+1}) \end{aligned}$$

$$\begin{aligned}
\Delta V_k &= -2 \left(1 - \frac{\gamma \phi_k^T \phi_k}{\mathcal{N}_k} \right) \frac{\tilde{\theta}_{k+1}^T \nabla L_k(\theta_{k+1})}{\mathcal{N}_k} \\
&\quad + \frac{1}{\gamma} \|\bar{\theta}_k - \vartheta_k\|^2 - \frac{1}{\gamma} \|\theta_k - \vartheta_k\|^2 - \frac{\beta(2-\beta)}{\gamma} \|\bar{\theta}_k - \vartheta_k\|^2 \\
&\quad + \frac{4}{\mathcal{N}_k} (1-\beta) (\bar{\theta}_k - \vartheta_k)^T \nabla L_k(\theta_{k+1}) \\
\Delta V_k &= -2 \left(1 - \frac{\gamma \phi_k^T \phi_k}{\mathcal{N}_k} \right) \frac{\tilde{\theta}_{k+1}^T \nabla L_k(\theta_{k+1})}{\mathcal{N}_k} \\
&\quad + \frac{\gamma \beta^2}{\mathcal{N}_k^2} \|\nabla L_k(\theta_k)\|^2 - \frac{2\beta}{\mathcal{N}_k} (\theta_k - \vartheta_k)^T \nabla L_k(\theta_k) \\
&\quad - \frac{\beta(2-\beta)}{\gamma} \|\bar{\theta}_k - \vartheta_k\|^2 + \frac{4}{\mathcal{N}_k} (1-\beta) (\bar{\theta}_k - \vartheta_k)^T \nabla L_k(\theta_{k+1}) \\
\Delta V_k &= \frac{1}{\mathcal{N}_k} \left\{ -2 \left(1 - \frac{\gamma \phi_k^T \phi_k}{\mathcal{N}_k} \right) \tilde{\theta}_{k+1}^T \nabla L_k(\theta_{k+1}) + \frac{\gamma \beta^2}{\mathcal{N}_k} \|\nabla L_k(\theta_k)\|^2 - 2\beta (\theta_k - \vartheta_k)^T \nabla L_k(\theta_k) \right. \\
&\quad \left. - \frac{\beta(2-\beta)\mathcal{N}_k}{\gamma} \|\bar{\theta}_k - \vartheta_k\|^2 + 4(1-\beta) (\bar{\theta}_k - \vartheta_k)^T \nabla L_k(\theta_{k+1}) \right\} \\
\Delta V_k &= \frac{1}{\mathcal{N}_k} \left\{ -2 \left(1 - \frac{\gamma \phi_k^T \phi_k}{\mathcal{N}_k} \right) \tilde{\theta}_{k+1}^T \nabla L_k(\theta_{k+1}) - \frac{\gamma \beta^2}{\mathcal{N}_k} \|\nabla L_k(\theta_k)\|^2 - 2\beta (\bar{\theta}_k - \vartheta_k)^T \nabla L_k(\theta_k) \right. \\
&\quad \left. - \frac{\beta(2-\beta)\mathcal{N}_k}{\gamma} \|\bar{\theta}_k - \vartheta_k\|^2 + 4(1-\beta) (\bar{\theta}_k - \vartheta_k)^T \nabla L_k(\theta_{k+1}) \right\} \\
\Delta V_k &= \frac{1}{\mathcal{N}_k} \left\{ -2 \left(1 - \frac{\gamma \phi_k^T \phi_k}{\mathcal{N}_k} \right) \tilde{\theta}_{k+1}^T \nabla L_k(\theta_{k+1}) - \frac{\gamma \beta^2}{\mathcal{N}_k} \|\nabla L_k(\theta_k)\|^2 - 2\beta (\bar{\theta}_k - \vartheta_k)^T \phi_k \phi_k^T \tilde{\theta}_k \right. \\
&\quad \left. - \frac{\beta(2-\beta)\mathcal{N}_k}{\gamma} \|\bar{\theta}_k - \vartheta_k\|^2 + 4(1-\beta) (\bar{\theta}_k - \vartheta_k)^T \nabla L_k(\theta_{k+1}) \right\} \\
\Delta V_k &= \frac{1}{\mathcal{N}_k} \left\{ -2 \left(1 - \frac{\gamma \phi_k^T \phi_k}{\mathcal{N}_k} \right) \tilde{\theta}_{k+1}^T \nabla L_k(\theta_{k+1}) - \frac{\gamma \beta^2}{\mathcal{N}_k} \|\nabla L_k(\theta_k)\|^2 \right. \\
&\quad \left. - \frac{\beta(2-\beta)\mathcal{N}_k}{\gamma} \|\bar{\theta}_k - \vartheta_k\|^2 + 4(1-\beta) (\bar{\theta}_k - \vartheta_k)^T \nabla L_k(\theta_{k+1}) \right. \\
&\quad \left. - 2\beta (\bar{\theta}_k - \vartheta_k)^T \phi_k \phi_k^T [\theta_k - \theta^* + (1-\beta)\bar{\theta}_k + \beta\vartheta_k - (1-\beta)\bar{\theta}_k - \beta\vartheta_k] \right\} \\
\Delta V_k &= \frac{1}{\mathcal{N}_k} \left\{ -2 \left(1 - \frac{\gamma \phi_k^T \phi_k}{\mathcal{N}_k} \right) \tilde{\theta}_{k+1}^T \nabla L_k(\theta_{k+1}) - \frac{\gamma \beta^2}{\mathcal{N}_k} \|\nabla L_k(\theta_k)\|^2 \right. \\
&\quad \left. - 2\beta (\bar{\theta}_k - \vartheta_k)^T \nabla L_k(\theta_{k+1}) - \frac{\beta(2-\beta)\mathcal{N}_k}{\gamma} \|\bar{\theta}_k - \vartheta_k\|^2 \right. \\
&\quad \left. + 4(1-\beta) (\bar{\theta}_k - \vartheta_k)^T \nabla L_k(\theta_{k+1}) - 2\beta (\bar{\theta}_k - \vartheta_k)^T \phi_k \phi_k^T [\theta_k - \bar{\theta}_k + \beta(\bar{\theta}_k - \vartheta_k)] \right\}
\end{aligned}$$

$$\begin{aligned}
\Delta V_k &= \frac{1}{\mathcal{N}_k} \left\{ -2 \left(1 - \frac{\gamma \phi_k^T \phi_k}{\mathcal{N}_k} \right) \tilde{\theta}_{k+1}^T \nabla L_k(\theta_{k+1}) - \frac{\gamma \beta^2}{\mathcal{N}_k} \|\nabla L_k(\theta_k)\|^2 \right. \\
&\quad - 2\gamma \beta^2 (\bar{\theta}_k - \vartheta_k)^T \frac{\phi_k \phi_k^T}{\mathcal{N}_k} \nabla L_k(\theta_k) - \frac{\beta(2-\beta)\mathcal{N}_k}{\gamma} \|\bar{\theta}_k - \vartheta_k\|^2 \\
&\quad \left. + 4(1 - \frac{3}{2}\beta)(\bar{\theta}_k - \vartheta_k)^T \nabla L_k(\theta_{k+1}) - 2\beta^2 (\bar{\theta}_k - \vartheta_k)^T \phi_k \phi_k^T (\bar{\theta}_k - \vartheta_k) \right\} \\
\Delta V_k &\leq \frac{1}{\mathcal{N}_k} \left\{ -2 \left(1 - \frac{\gamma \phi_k^T \phi_k}{\mathcal{N}_k} \right) \tilde{\theta}_{k+1}^T \nabla L_k(\theta_{k+1}) - 16 \|\phi_k\|^2 \|\bar{\theta}_k - \vartheta_k\|^2 \right. \\
&\quad + 4(1 - \frac{3}{2}\beta)(\bar{\theta}_k - \vartheta_k)^T \nabla L_k(\theta_{k+1}) \\
&\quad - \frac{\gamma \beta^2}{\mathcal{N}_k} \|\nabla L_k(\theta_k)\|^2 - \beta^2 \|\phi_k\|^2 \|\bar{\theta}_k - \vartheta_k\|^2 - 2\beta^2 (\bar{\theta}_k - \vartheta_k)^T \gamma \frac{\phi_k \phi_k^T}{\mathcal{N}_k} \nabla L_k(\theta_k) \\
&\quad \left. - (16 + \beta^2) \|\bar{\theta}_k - \vartheta_k\|^2 - 2\beta^2 (\bar{\theta}_k - \vartheta_k)^T \phi_k \phi_k^T (\bar{\theta}_k - \vartheta_k) \right\} \\
\Delta V_k &\leq \frac{1}{\mathcal{N}_k} \left\{ -\frac{30}{16} \|\tilde{\theta}_{k+1}^T \phi_k\|^2 - 16 \|\phi_k\|^2 \|\bar{\theta}_k - \vartheta_k\|^2 + 8 \|\bar{\theta}_k - \vartheta_k\| \|\phi_k\| \|\tilde{\theta}_{k+1}^T \phi_k\| \right. \\
&\quad - \frac{\gamma \beta^2}{\mathcal{N}_k} \|\nabla L_k(\theta_k)\|^2 - \beta^2 \|\phi_k\|^2 \|\bar{\theta}_k - \vartheta_k\|^2 + 2\beta^2 \|\bar{\theta}_k - \vartheta_k\| \frac{\|\sqrt{\gamma} \phi_k\|^2}{\mathcal{N}_k} \|\nabla L_k(\theta_k)\| \\
&\quad \left. - (16 + \beta^2) \|\bar{\theta}_k - \vartheta_k\|^2 - 2\beta^2 (\bar{\theta}_k - \vartheta_k)^T \phi_k \phi_k^T (\bar{\theta}_k - \vartheta_k) \right\} \\
\Delta V_k &\leq \frac{1}{\mathcal{N}_k} \left\{ -\|\tilde{\theta}_{k+1}^T \phi_k\|^2 - 16 \|\phi_k\|^2 \|\bar{\theta}_k - \vartheta_k\|^2 + 8 \|\bar{\theta}_k - \vartheta_k\| \|\phi_k\| \|\tilde{\theta}_{k+1}^T \phi_k\| \right. \\
&\quad - \frac{\gamma \beta^2}{\mathcal{N}_k} \|\nabla L_k(\theta_k)\|^2 - \beta^2 \|\phi_k\|^2 \|\bar{\theta}_k - \vartheta_k\|^2 + \frac{2\sqrt{\gamma} \beta^2}{\sqrt{\mathcal{N}_k}} \|\bar{\theta}_k - \vartheta_k\| \|\phi_k\| \|\nabla L_k(\theta_k)\| \\
&\quad \left. - \frac{7}{8} \|\tilde{\theta}_{k+1}^T \phi_k\|^2 - (16 + \beta^2) \|\bar{\theta}_k - \vartheta_k\|^2 - 2\beta^2 (\bar{\theta}_k - \vartheta_k)^T \phi_k \phi_k^T (\bar{\theta}_k - \vartheta_k) \right\} \\
\Delta V_k &\leq \frac{1}{\mathcal{N}_k} \left\{ - \left[\|\tilde{\theta}_{k+1}^T \phi_k\| - 4 \|\phi_k\| \|\bar{\theta}_k - \vartheta_k\| \right]^2 \right. \\
&\quad - \left[\frac{\sqrt{\gamma} \beta}{\sqrt{\mathcal{N}_k}} \|\nabla L_k(\theta_k)\| - \beta \|\phi_k\| \|\bar{\theta}_k - \vartheta_k\| \right]^2 \\
&\quad \left. - \frac{7}{8} \|\tilde{\theta}_{k+1}^T \phi_k\|^2 - (16 + \beta^2) \|\bar{\theta}_k - \vartheta_k\|^2 - 2\beta^2 \|(\bar{\theta}_k - \vartheta_k)^T \phi_k\|^2 \right\} \leq 0.
\end{aligned}$$

Thus it can be concluded that V is a Lyapunov function with $(\theta - \theta^*) \in \ell_\infty$ and $(\theta - \vartheta) \in \ell_\infty$. Using (27) and \mathcal{N}_k from equations (61)-(63), $\frac{\epsilon_{y,k}}{\mathcal{N}_k} \in \ell_\infty$. Collecting ΔV_k terms from t_0 to T : $\sum_{k=t_0}^T \frac{7}{4} \|\sqrt{\frac{L_k(\theta_{k+1})}{\mathcal{N}_k}}\|^2 \leq V_{t_0} - V_{T+1} < \infty$. Taking $T \rightarrow \infty$, it can be seen that $\sqrt{\frac{L_k(\theta_{k+1})}{\mathcal{N}_k}} \in \ell_2 \cap \ell_\infty$ and therefore $\lim_{k \rightarrow \infty} \sqrt{\frac{L_k(\theta_{k+1})}{\mathcal{N}_k}} = 0$. If additionally $\phi \in \ell_\infty$, then $\sqrt{L_k(\theta_{k+1})} \in \ell_2 \cap \ell_\infty$ and therefore $\lim_{k \rightarrow \infty} \sqrt{L_k(\theta_{k+1})} = 0$ and $\lim_{k \rightarrow \infty} L_k(\theta_{k+1}) = 0$. \square

6.5 Proof for Lemma 1

Proof. The normalized loss function gap may be bounded from above using f in (34), $\Psi \geq \max\{1, \|\theta_0 - \theta^*\|^2\}$, and $\mu = \epsilon/\Psi$ as

$$\begin{aligned} \frac{L(\theta_k) - L(\theta^*)}{\mathcal{N}} &= f(\theta_k) - f(\theta^*) \\ &\quad + \frac{\mu}{2} (\|\theta^* - \theta_0\|^2 - \|\theta_k - \theta_0\|^2) \\ &\leq f(\theta_k) - f(\theta_\epsilon^*) + \frac{\epsilon}{2}, \end{aligned}$$

where $f(\theta_\epsilon^*)$ is the optimal value of f , that is, $\nabla f(\theta_\epsilon^*) = \frac{\nabla L(\theta_\epsilon^*)}{\mathcal{N}} + \mu(\theta_\epsilon^* - \theta_0) = 0$. Applying the result of Theorem 5 to f in (34) with $\Psi \geq \max\{1, \|\theta_0 - \theta^*\|^2\}$, $\mu = \epsilon/\Psi$, $\bar{L} = 1 + \mu$, $\bar{\alpha} = 1/\bar{L}$, $\kappa = \bar{L}/\mu$, $\bar{\beta}_k = (\sqrt{\kappa} - 1)/(\sqrt{\kappa} + 1)$, the normalized loss function gap may be bounded as

$$\begin{aligned} \frac{L(\theta_k) - L(\theta^*)}{\mathcal{N}} &\leq \frac{\bar{L} + \mu}{2} \|\theta_0 - \theta_\epsilon^*\|^2 \exp\left(-\frac{k}{\sqrt{\kappa}}\right) + \frac{\epsilon}{2} \\ &\leq \frac{\bar{L} + \mu}{2} \|\theta_0 - \theta^*\|^2 \exp\left(-\frac{k}{\sqrt{\kappa}}\right) + \frac{\epsilon}{2} \\ &= \frac{\Psi + 2\epsilon}{2\Psi} \|\theta_0 - \theta^*\|^2 \exp\left(-\frac{k}{\sqrt{\kappa}}\right) + \frac{\epsilon}{2} \\ &\leq \frac{\Psi + 2\epsilon}{2} \exp\left(-\frac{k}{\sqrt{\kappa}}\right) + \frac{\epsilon}{2} \\ &= \frac{\Psi + 2\epsilon}{2} \exp\left(-\frac{k}{\sqrt{1 + \frac{\Psi}{\epsilon}}}\right) + \frac{\epsilon}{2} \end{aligned}$$

Thus $\frac{L(\theta_k) - L(\theta^*)}{\mathcal{N}} \leq \epsilon$ if,

$$k \geq \left\lceil \sqrt{1 + \frac{\Psi}{\epsilon}} \log\left(2 + \frac{\Psi}{\epsilon}\right) \right\rceil.$$

□

6.6 Proof for Lemma 2

Proof. The loss function gap may be bounded from above using f in (34), $\Psi \geq \max\{1, \mathcal{N}\|\theta_0 - \theta^*\|^2\}$, and $\mu = \epsilon/\Psi$ as

$$\begin{aligned} L(\theta_k) - L(\theta^*) &= \mathcal{N}(f(\theta_k) - f(\theta^*)) \\ &\quad + \frac{\mu}{2} \mathcal{N} (\|\theta^* - \theta_0\|^2 - \|\theta_k - \theta_0\|^2) \\ &\leq \mathcal{N}(f(\theta_k) - f(\theta_\epsilon^*)) + \frac{\epsilon}{2}, \end{aligned}$$

where $f(\theta_\epsilon^*)$ is the optimal value of f , that is, $\nabla f(\theta_\epsilon^*) = \frac{\nabla L(\theta_\epsilon^*)}{\mathcal{N}} + \mu(\theta_\epsilon^* - \theta_0) = 0$. Applying the result of Theorem 5 to f in (34) with $\Psi \geq \max\{1, \mathcal{N}\|\theta_0 - \theta^*\|^2\}$, $\mu = \epsilon/\Psi$, $\bar{L} = 1 + \mu$,

$\bar{\alpha} = 1/\bar{L}$, $\kappa = \bar{L}/\mu$, $\bar{\beta}_k = (\sqrt{\kappa} - 1)/(\sqrt{\kappa} + 1)$, the loss function gap may be bounded as

$$\begin{aligned}
L(\theta_k) - L(\theta^*) &\leq \frac{\bar{L} + \mu}{2} \mathcal{N} \|\theta_0 - \theta_\epsilon^*\|^2 \exp\left(-\frac{k}{\sqrt{\kappa}}\right) + \frac{\epsilon}{2} \\
&\leq \frac{\bar{L} + \mu}{2} \mathcal{N} \|\theta_0 - \theta^*\|^2 \exp\left(-\frac{k}{\sqrt{\kappa}}\right) + \frac{\epsilon}{2} \\
&= \frac{\Psi + 2\epsilon}{2\Psi} \mathcal{N} \|\theta_0 - \theta^*\|^2 \exp\left(-\frac{k}{\sqrt{\kappa}}\right) + \frac{\epsilon}{2} \\
&\leq \frac{\Psi + 2\epsilon}{2} \exp\left(-\frac{k}{\sqrt{\kappa}}\right) + \frac{\epsilon}{2} \\
&= \frac{\Psi + 2\epsilon}{2} \exp\left(-\frac{k}{\sqrt{1 + \frac{\Psi}{\epsilon}}}\right) + \frac{\epsilon}{2}
\end{aligned}$$

Thus $L(\theta_k) - L(\theta^*) \leq \epsilon$ if,

$$k \geq \left\lceil \sqrt{1 + \frac{\Psi}{\epsilon}} \log\left(2 + \frac{\Psi}{\epsilon}\right) \right\rceil.$$

□

6.7 Proof for Theorem 6

Proof. For the same function V as in (96) and ΔV_k , by taking expectation using (27), (28), and the update law in (61)-(63) we obtain

$$\begin{aligned}
&E(V_{k+1}|\mathcal{F}_k) - V_k \\
&\leq - \underbrace{\frac{10}{16}\mu\gamma\beta V_k}_{c_1} + \underbrace{\frac{19609}{6144}d_{max}\sqrt{V_k}}_{c_2} \\
&\quad + \underbrace{\mu\left(\frac{3570\beta + 896}{224\beta}\right)\|\theta^* - \theta_0\|^2}_{c_3} \\
&\quad + \underbrace{\frac{67}{256}d_{max}\|\theta_0\| + \frac{1}{8}d_{max}\|(\theta^* - \theta_0)\| + \frac{15001}{1536}d_{max}\|\theta^*\|}_{c_4} \\
&\quad + \underbrace{4\gamma\beta\sigma_{max}^2\left|1 - \frac{3}{2}\beta\right| + 2(1 - \beta)\gamma\beta\sigma_{max}^2 + 2\gamma\sigma_{max}^2}_{c_5}. \tag{97}
\end{aligned}$$

Derivation of (97) is based on straightforward, yet tedious, algebraic manipulations which can be found in pages 8-28 of [51]. Defining the compact set D as

$$D = \{V | V \leq K\}$$

where $\hat{c} = c_3 + c_4 + c_5$ and K is the greatest positive real root of $-c_1x + c_2\sqrt{x} + \hat{c} = 0$, the inequality in (97) can be shown to satisfy

$$E(V_{k+1}|\mathcal{F}_k) - V_k < 0, \tag{98}$$

in D^c . In order to show the properties of V_k outside of the compact set D , we consider a new function \hat{V}_k , defined as

$$\hat{V}(x_k) = \hat{V}_k = \begin{cases} V_k - K & V_k > K \\ 0 & V_k \leq K \end{cases} \quad (99)$$

Since $0 < \alpha < c_1$, it follows that whenever $V_k > \frac{c_2^2}{(\alpha - c_1)^2}$, the following holds,

$$(\alpha - c_1)V_k + c_2\sqrt{V_k} \leq 0$$

From this we can conclude that

$$E(V_{k+1}|\mathcal{F}_k) - V_k \leq -\alpha V_k + \hat{c}, \quad \forall V_k \in S^c$$

where

$$S = \left\{ V \mid V \leq \frac{c_2^2}{(\alpha - c_1)^2} \right\}.$$

We can additionally conclude that $E(V_{k+1}|\mathcal{F}_k) - V_k < 0$ whenever V_k is in $S^c \cap F^c$ where

$$F = \left\{ V \mid V \leq \frac{\hat{c}}{\alpha} \right\}$$

Since $S^c \cap F^c = (S \cup F)^c$ by Demorgan's law, it follows that if

$$G = \left\{ V \mid V \leq \frac{c_2^2}{(\alpha - c_1)^2} \vee V \leq \frac{\hat{c}}{\alpha} \right\} \quad (100)$$

and $K = \max\{\frac{c_2^2}{(\alpha - c_1)^2}, \frac{\hat{c}}{\alpha}\}$, G is equivalent to

$$G = \{V \mid V \leq K\}.$$

Define $\hat{V}(x_k)$ as in (99). Now we show that

$$E(\hat{V}_{k+1}|\mathcal{F}_k) - \hat{V}_k \leq -\alpha\hat{V}_k, \quad \forall k, \quad (101)$$

by considering two cases:

1. $\hat{V}_k > 0$: This means that $V_k > K$. Thus $V_k \in G^c$, which means that $E(V_{k+1}|\mathcal{F}_k) - V_k \leq -\alpha V_k + \hat{c}$. Since in this case $\hat{V}_k = V_k - K$, it follows that $E(V_{k+1}|\mathcal{F}_k) - V_k \leq -\alpha\hat{V}_k - \alpha K + \hat{c}$. Additionally, since $K \geq \frac{\hat{c}}{\alpha}$, it follows that $E(V_{k+1}|\mathcal{F}_k) - V_k \leq -\alpha\hat{V}_k$. By adding and subtracting K , we get $E(V_{k+1} - K|\mathcal{F}_k) - (V_k - K) \leq -\alpha\hat{V}_k$. Since $\hat{V}_k > 0$, we have $E(V_{k+1} - K|\mathcal{F}_k) - \hat{V}_k \leq -\alpha\hat{V}_k$. We now consider two subcases depending on V_{k+1} :
 - (a) $V_{k+1} > K$: In this case, $E(\hat{V}_{k+1}|\mathcal{F}_k) = E(V_{k+1} - K|\mathcal{F}_k)$. Hence $E(\hat{V}_{k+1}|\mathcal{F}_k) - \hat{V}_k \leq -\alpha\hat{V}_k$.
 - (b) $V_{k+1} \leq K$: In this case, $\hat{V}_{k+1} = 0$. This implies that $E(\hat{V}_{k+1}|\mathcal{F}_k) = 0$ and $E(\hat{V}_{k+1}|\mathcal{F}_k) - \hat{V}_k \leq -\alpha\hat{V}_k$ because $\alpha < 1$.

Therefore we conclude in case 1) that $E(\hat{V}_{k+1}|\mathcal{F}_k) - \hat{V}_k \leq -\alpha\hat{V}_k$.

2. $\hat{V}_k = 0$: This means $V_k \leq K$. We know that $E(V_{k+1}|\mathcal{F}_k) - V_k \leq -c_1V_k + c_2\sqrt{V_k} + \hat{c}$. We can conclude then that $E(V_{k+1}|\mathcal{F}_k) \leq (1 - c_1)V_k + c_2\sqrt{V_k} + \hat{c}$. Since we also have that $1 - c_1 > 0$, we can conclude that $E(V_{k+1}|\mathcal{F}_k) \leq (1 - c_1)K + c_2\sqrt{K} + \hat{c}$. Since $K \geq \frac{c_2^2}{(\alpha - c_1)^2}$, we can conclude that $-c_1K + c_2\sqrt{K} \leq -\alpha K$. Thus we get $E(V_{k+1}|\mathcal{F}_k) \leq -\alpha K + \hat{c} + K$. And as shown above, $-\alpha K \leq -\hat{c}$. Thus, $E(V_{k+1}|\mathcal{F}_k) \leq K$. This then implies that $E(\hat{V}_{k+1}|\mathcal{F}_k) = 0$. Thus once again we get $E(\hat{V}_{k+1}|\mathcal{F}_k) - \hat{V}_k \leq -\alpha\hat{V}_k$.

This implies that $E(\hat{V}(x_{k+1}|\mathcal{F}_k) - \hat{V}(x_k)) \leq -\alpha\hat{V}(x_k)$, $\forall x_k \in \mathbb{R}^n$. We therefore apply Theorem 2 in [51] to guarantee that $\hat{V}(x_k)$ converges to zero exponentially at a rate no slower than $1 - \alpha$. This implies that $V(x_k)$ converges to the set G at the same exponential rate. \square

6.8 Proof for Lemma 3

Proof. Using convolution, Ω_k can be rewritten as

$$\Omega_k = (1 - \lambda_\Omega)^k \Omega_0 + \sum_{i=0}^{k-1} (1 - \lambda_\Omega)^{k-i-1} \frac{\phi_i \phi_i^T}{1 + \|\phi_i\|^2}$$

Since ϕ_k is persistently exciting,

$$\begin{aligned} \Omega_k &\succeq (1 - \lambda_\Omega)^{k-1} \sum_{i=k-\Delta T}^{k-1} (1 - \lambda_\Omega)^{-i} \frac{\phi_i \phi_i^T}{1 + \|\phi_i\|^2} \\ &\succeq \Omega_{PEI} \end{aligned}$$

\square

6.9 Proof for Lemma 4

Proof. We first consider the scalar case of (83), given by

$$\gamma_k = \gamma_{k-1} + \lambda_\Gamma(\gamma_{k-1} - \kappa\omega_k\gamma_{k-1}^2), \quad (102)$$

where

$$0 < \omega_{\min} \leq \omega_k \leq \omega_{\max}. \quad (103)$$

Let $\gamma_{\max} > 0$ and

$$\gamma_{\min} = \min \left\{ \frac{1}{\kappa\omega_{\max}}, \gamma_{\max} + \lambda_\Gamma(\gamma_{\max} - \kappa\omega_{\max}\gamma_{\max}^2) \right\} \quad (104)$$

where $\kappa_{\min} \leq \kappa < \kappa_{\max}$, and κ_{\min} , κ_{\max} are defined as

$$\kappa_{\min} = \frac{1}{\gamma_{\max}\omega_{\min}}, \quad \kappa_{\max} = \frac{1 + \lambda_\Gamma}{\lambda_\Gamma\omega_{\max}\gamma_{\max}}. \quad (105)$$

In the update of (102), γ_{\max} and λ_Γ are chosen arbitrarily by the user. The gain κ is then chosen using the bounds in (105). We now state the following lemma that establishes bounds of γ_k which in turn depend on λ_Γ , γ_{\max} and κ .

We can show the following result: *If $0 < \lambda_\Gamma < \min \left\{ \frac{1}{\omega_{\max}/\omega_{\min}-1}, 1 \right\}$, and $\gamma_{\min} \leq \gamma_0 \leq \gamma_{\max}$, then the solutions of (102) are such that $0 < \gamma_{\min} \leq \gamma_k \leq \gamma_{\max}$, $\forall k \geq 0$.*

Defining the right hand side of Eq. (44) as $f(\gamma_{k-1}, \omega_k)$, it is easy to see that $f(.,.)$ is quadratic in γ_{k-1} , with one maximum and two minima. Suppose ω^* is such that

$$\frac{1 + \lambda_\Gamma}{2\lambda_\Gamma \kappa \omega^*} = \gamma_{\max}. \quad (106)$$

It is easy to check that $\omega^* \geq \omega_{\min}$. If $\omega_k \geq \omega^*$,

$$\begin{aligned} f(\gamma_{k-1}, \omega_k) &\leq \gamma_{\max} + \lambda_\Gamma(\gamma_{\max} - \kappa\omega^*\gamma_{\max}^2) \\ &\leq \gamma_{\max} + \lambda_\Gamma(\gamma_{\max} - \kappa\omega_{\min}\gamma_{\max}^2). \end{aligned}$$

If $\omega_k \leq \omega^*$,

$$\begin{aligned} f(\gamma_{k-1}, \omega_k) &\leq \gamma_{\max} + \lambda_\Gamma(\gamma_{\max} - \kappa\omega_k\gamma_{\max}^2) \\ &\leq \gamma_{\max} + \lambda_\Gamma(\gamma_{\max} - \kappa\omega_{\min}\gamma_{\max}^2). \end{aligned}$$

Noticing the bounds of λ_Γ and κ , simple algebraic manipulations show that

$$\begin{aligned} \max_{\gamma_k, \omega_k} f(\gamma_{k-1}, \omega_k) &= \gamma_{\max} + \lambda_\Gamma(\gamma_{\max} - \kappa\omega_{\min}\gamma_{\max}^2) \\ &\leq \gamma_{\max}. \end{aligned}$$

Similarly, it can be shown by inspection that

$$\min_{\omega_k} f(\gamma_{k-1}, \omega_k) = \gamma_{k-1} + \lambda_\Gamma(\gamma_{k-1} - \kappa\omega_{\max}\gamma_{k-1}^2).$$

Since the largest decrease of f occurs when γ_k is at its maximum value, it follows that

$$\min_{\gamma_k, \omega_k} f(\gamma_{k-1}, \omega_k) = \gamma_{\max} + \lambda_\Gamma(\gamma_{\max} - \kappa\omega_{\max}\gamma_{\max}^2).$$

In addition, $\kappa\omega_{\max} > 0$. Therefore, the lower bound of γ_k and that it is positive are ensured through the choice of γ_{\min} as in (104).

We then establish the lower bound Γ_{PE} using induction: Let $\Gamma_{PE}I \preceq \Gamma_{k-1} \preceq \Gamma_{\max}I$. It is easy to check that $\Gamma_{PE} > 0$. Since Γ_{k-1} is positive definite, we can factorize Γ_{k-1} as

$$\Gamma_{k-1} = Q_{k-1}\Lambda_{k-1}Q_{k-1}^\top \quad (107)$$

where Λ_{k-1} is diagonal and all of its entries are the eigenvalues of Γ_{k-1} , and Q_{k-1} is orthogonal. Using Eq. (83) and the fact that Q_{k-1} is orthogonal, we obtain that

$$\begin{aligned} \Gamma_k &= \Gamma_{k-1} + \lambda_\Gamma(\Gamma_{k-1} - \kappa\Gamma_{k-1}\Omega_k\Gamma_{k-1}) \\ &\succeq \Gamma_{k-1} + \lambda_\Gamma(\Gamma_{k-1} - \kappa\Omega_{\max}\Gamma_{k-1}^2) \\ &= Q_{k-1} \left[\Lambda_{k-1} + \lambda_\Gamma(\Lambda_{k-1} - \kappa\Omega_{\max}\Lambda_{k-1}^2) \right] Q_{k-1}^\top, \end{aligned}$$

since

$$x^\top(\Omega_{\max}I - \Omega_k)x \geq 0, \quad \forall x \neq 0.$$

Since Γ_{k-1} is positive definite, it follows that

$$v^\top \Gamma_{k-1} (\Omega_{\max} I - \Omega_k) \Gamma_{k-1} v \geq 0, \quad \forall v \neq 0.$$

Thus

$$\Gamma_{k-1} (\Omega_{\max} I - \Omega_k) \Gamma_{k-1} \succeq 0. \quad (108)$$

Denote the i th diagonal element of Γ_{k-1} as $\lambda_{k-1,i}$, $i = 1, \dots, N$. Since $\Gamma_{PE} I \preceq \Gamma_{k-1} \preceq \Gamma_{\max} I$, we have $\Gamma_{PE} \leq \lambda_{k-1,i} \leq \Gamma_{\max}$, $\forall i$. From the above boundedness results for (102), the same bounds then hold for λ_i as well, i.e., $\Gamma_{PE} \leq \lambda_{k,i} \leq \Gamma_{\max}$, $\forall i$ and the lower bound of Γ_k is proved. Since the lower bound holds for $k = k_2$, proof by induction guarantees that the lower bound holds for all $k \geq k_2$.

To prove the upper bound, similar to Eq. (108), using Lemma 3 we can show that

$$\Gamma_{k-1} (\Omega_{PE} I - \Omega_k) \Gamma_{k-1} \preceq 0. \quad (109)$$

Therefore

$$\Gamma_k \preceq Q_{k-1} [\Lambda_{k-1} + \lambda_\Gamma (\Lambda_{k-1} - \kappa \Omega_{PE} \Lambda_{k-1}^2)] Q_{k-1}^\top.$$

Using the same procedure as above, it can be shown that the upper bound holds for Γ_k if it holds for Γ_{k-1} , and using induction that the upper bound holds for all k , Lemma 4 is proved. \square

6.10 Proof for Theorem 9

Proof. Starting from (81), we get

$$\theta_k - \theta^* = \left(I - \frac{\lambda_\Gamma \kappa \Gamma_{k-1} \phi_{k-1} \phi_{k-1}^\top}{1 + \|\phi_{k-1}\|^2} \right) \tilde{\theta}_{k-1}. \quad (110)$$

Using (89), we rewrite Γ_k as

$$\Gamma_k = \bar{\Gamma}_k + \underbrace{\lambda_\Gamma \Gamma_{k-1} - \lambda_\Gamma \kappa (1 - \lambda_\Omega) \Gamma_{k-1} \Omega_{k-1} \Gamma_{k-1}}_{\Upsilon_k} \quad (111)$$

Now we show that under the conditions in Theorem 9, $\bar{\Gamma}_k \succeq \bar{\Gamma}_{\min} I \succ 0$. With simple manipulations, it can be shown that

$$\bar{\Gamma}_k \succeq Q_{k-1} (\Lambda_{k-1} - \lambda_\Gamma \kappa \Lambda_{k-1}^2) Q_{k-1}^\top. \quad (112)$$

It is easy to see that $\Gamma_{PE} \leq \lambda_{k-1,i} \leq \Gamma_{\max}$, $\forall i$, where $\lambda_{k-1,i}$ is the i th diagonal element of Γ_{k-1} . From the inequality in (112), $\bar{\Gamma}_k$ assumes its lower bound either when $\lambda_{k-1,i} = \Gamma_{PE}$ or when $\lambda_{k-1,i} = \Gamma_{\max}$. It follows therefore that $\bar{\Gamma}_k \succeq \bar{\Gamma}_{\min} I$, where $\bar{\Gamma}_{\min} > 0$ is defined as

$$\bar{\Gamma}_{\min} = \min \{ \Gamma_{\max} - \lambda_\Gamma \kappa \Gamma_{\max}^2, \Gamma_{PE} - \lambda_\Gamma \kappa \Gamma_{PE}^2 \}. \quad (113)$$

It is also obvious that $\bar{\Gamma}_k \preceq \bar{\Gamma}_{\max} I$, where $\bar{\Gamma}_{\max} = \Gamma_{\max}$. Using the same approach, we can also show that $0 \prec \Upsilon_{\min} I \preceq \Upsilon_k \preceq \Upsilon_{\max} I$, where Υ_k is defined in (111) and $\Upsilon_{\max} = \lambda_\Gamma \Gamma_{\max}$. With

these bounds established, we consider the Lyapunov function in (90). Since $\tilde{\theta}_k = \bar{\Gamma}_k \Gamma_{k-1}^{-1} \tilde{\theta}_{k-1}$, we obtain that

$$\begin{aligned} V_k &= \left(\bar{\Gamma}_k \Gamma_{k-1}^{-1} \tilde{\theta}_{k-1} \right)^T \bar{\Gamma}_k^{-1} \\ &\quad \left[\left(I - \lambda_{\Gamma} \kappa \frac{\Gamma_{k-1} \phi_{k-1} \phi_{k-1}^T}{1 + \|\phi_{k-1}\|^2} \right) \tilde{\theta}_{k-1} \right] \\ &= \tilde{\theta}_{k-1}^T \Gamma_{k-1}^{-1} \tilde{\theta}_{k-1} - \lambda_{\Gamma} \kappa \frac{\tilde{\theta}_{k-1} \phi_{k-1} \phi_{k-1} \tilde{\theta}_{k-1}}{1 + \|\phi_{k-1}\|^2}. \end{aligned}$$

Since $\Upsilon_k \succ 0$, we can write $\Upsilon_k = \Upsilon_k^{1/2} \Upsilon_k^{1/2}$. Applying matrix inversion lemma to (111), we have

$$\Gamma_k^{-1} = \bar{\Gamma}_k^{-1} - \underbrace{\bar{\Gamma}_k^{-1} \Upsilon_k^{1/2} \left(I + \Upsilon_k^{1/2} \bar{\Gamma}_k^{-1} \Upsilon_k^{1/2} \right)^{-1} \Upsilon_k^{1/2} \bar{\Gamma}_k^{-1}}_{\Psi_k}. \quad (114)$$

Since $\Upsilon_k^{1/2} \succ 0$ and $\bar{\Gamma}_k^{-1} \succ 0$, applying the definition of positive definite matrices we obtain that $\Upsilon_k^{1/2} \bar{\Gamma}_k^{-1} \Upsilon_k^{1/2} \succ 0$. Also, it follows that $\Upsilon_k^{1/2} \bar{\Gamma}_k^{-1} \Upsilon_k^{1/2} \preceq \lambda_{\Gamma} \bar{\Gamma}_{\min}^{-1} \Gamma_{\max} I$. Therefore $\left(I + \Upsilon_k^{1/2} \bar{\Gamma}_k^{-1} \Upsilon_k^{1/2} \right)^{-1} \succeq (1 + \lambda_{\Gamma} \bar{\Gamma}_{\min}^{-1} \Gamma_{\max})^{-1} I$. Applying the definition of positive definite matrices again, we get $\Psi_k \succeq \Psi_{\min} I \succ 0$. Substitute Γ_k^{-1} in (114) into V_k , we get

$$\begin{aligned} V_k &= \tilde{\theta}_{k-1}^T \Gamma_{k-1}^{-1} \tilde{\theta}_{k-1} - \lambda_{\Gamma} \kappa \frac{\tilde{\theta}_{k-1} \phi_{k-1} \phi_{k-1} \tilde{\theta}_{k-1}}{1 + \|\phi_{k-1}\|^2} \\ &= \tilde{\theta}_{k-1}^T (\bar{\Gamma}_{k-1}^{-1} - \Psi_{k-1}) \tilde{\theta}_{k-1} \\ &\leq (1 - \underbrace{\Psi_{\min} \bar{\Gamma}_{\min}}_{\mu_1}) V_{k-1} \end{aligned} \quad (115)$$

where we have replaced $\tilde{\theta}_{k-1}$ with an upper bound involving V_{k-1} . From (114) and $\Gamma_k^{-1} \succ 0$, it follows that $\Psi_{\min} \bar{\Gamma}_{\min} < 1$. Therefore, we have

$$\begin{aligned} \Delta V_k &= V_k - V_{k-1} \\ &\leq -\mu_1 V_{k-1}, \end{aligned}$$

It can be noted that $\Delta V_k < 0$ when $V_{k-1} \neq 0$. For any k such that $V_k > 0$, it follows that

$$V_k \leq (1 - \mu_1) V_{k-1}$$

We therefore obtain that when $k \geq k_2$

$$\begin{aligned} V_k &\leq (1 - \mu_1)^{k-k_2} V_{k_2} \\ &\leq \exp[-\mu_1(k - k_2)] V_{k_2}. \end{aligned}$$

□

References

- [1] K. S. Narendra and A. M. Annaswamy, *Stable Adaptive Systems*. Dover, 2005.
- [2] P. A. Ioannou and J. Sun, *Robust Adaptive Control*. PTR Prentice-Hall, 1996.
- [3] S. Sastry and M. Bodson, *Adaptive Control: Stability, Convergence and Robustness*. Prentice-Hall, 1989.
- [4] J.-J. E. Slotine, W. Li *et al.*, *Applied nonlinear control*. Prentice hall Englewood Cliffs, NJ, 1991, vol. 199, no. 1.
- [5] M. Krstic, P. V. Kokotovic, and I. Kanellakopoulos, *Nonlinear and adaptive control design*. John Wiley & Sons, Inc., 1995.
- [6] A. Astolfi, D. Karagiannis, and R. Ortega, *Nonlinear and adaptive control with applications*. Springer Science & Business Media, 2007.
- [7] M. Guay and T. Zhang, “Adaptive extremum seeking control of nonlinear dynamic systems with parametric uncertainties,” *Automatica*, vol. 39, no. 7, pp. 1283–1293, 2003.
- [8] K. Zhou, J. C. Doyle, K. Glover *et al.*, *Robust and optimal control*. Prentice hall New Jersey, 1996, vol. 40.
- [9] K. Zhou and P. Khargonekar, “Stability robustness bounds for linear state-space models with structured uncertainty,” *IEEE Transactions on Automatic Control*, vol. 32, no. 7, pp. 621–623, 1987.
- [10] L. Hewing, K. P. Wabersich, M. Menner, and M. N. Zeilinger, “Learning-based model predictive control: Toward safe learning in control,” *Annual Review of Control, Robotics, and Autonomous Systems*, vol. 3, pp. 269–296, 2020.
- [11] J. B. Rawlings, D. Q. Mayne, and M. Diehl, *Model predictive control: theory, computation, and design*. Nob Hill Publishing Madison, WI, 2017, vol. 2.
- [12] V. I. Utkin, *Sliding modes in control and optimization*. Springer Science & Business Media, 2013.
- [13] B. Recht, “A tour of reinforcement learning: The view from continuous control,” *arXiv preprint arXiv:1806.09460*, 2018.
- [14] D. P. Bertsekas and J. N. Tsitsiklis, *Neuro-dynamic programming*. Athena Scientific, 1996.
- [15] R. S. Sutton and A. G. Barto, *Reinforcement learning: An introduction*. MIT press, 2018.
- [16] M. Vidyasagar, “Recent advances in reinforcement learning,” in *2020 American Control Conference (ACC)*. IEEE, 2020, pp. 4751–4756.
- [17] C. J. Watkins and P. Dayan, “Q-learning,” *Machine learning*, vol. 8, no. 3-4, pp. 279–292, 1992.

- [18] L. Ljung, *System Identification: Theory for the User*. Prentice-Hall, 1987.
- [19] G. C. Goodwin and K. S. Sin, *Adaptive Filtering Prediction and Control*. Prentice Hall, 1984.
- [20] K. J. Åström and B. Wittenmark, *Adaptive Control: Second Edition*. Addison-Wesley Publishing Company, 1995.
- [21] Y. Nesterov, *Lectures on Convex Optimization*. Springer International Publishing, 2018.
- [22] W. Su, S. Boyd, and E. J. Candès, “A differential equation for modeling nesterov’s accelerated gradient method: Theory and insights,” *Journal of Machine Learning Research*, vol. 17, no. 153, pp. 1–43, 2016.
- [23] A. Wibisono, A. C. Wilson, and M. I. Jordan, “A variational perspective on accelerated methods in optimization,” *Proceedings of the National Academy of Sciences*, vol. 113, no. 47, pp. E7351–E7358, 2016.
- [24] J. Zhang, A. Mokhtari, S. Sra, and A. Jadbabaie, “Direct runge-kutta discretization achieves acceleration,” *arXiv preprint arXiv:1805.00521*, 2018.
- [25] K. S. Narendra and A. M. Annaswamy, “Persistent excitation in adaptive systems,” *International Journal of Control*, vol. 45, no. 1, pp. 127–160, 1987.
- [26] P. A. Ioannou and P. V. Kokotovic, “Robust redesign of adaptive control,” *IEEE Transactions on Automatic Control*, vol. 29, no. 3, pp. 202–211, 1984.
- [27] K. J. Åström and B. Wittenmark, *Adaptive control*. Courier Corporation, 2013.
- [28] S. P. Karason and A. M. Annaswamy, “Adaptive control in the presence of input constraints,” *IEEE Transactions on Automatic Control*, vol. 39, no. 11, pp. 2325–2330, 1994.
- [29] E. Lavretsky and N. Hovakimyan, “Positive/spl mu/-modification for stable adaptation in the presence of input constraints,” in *Proceedings of the 2004 American Control Conference*, vol. 3. IEEE, 2004, pp. 2545–2550.
- [30] J. E. Gaudio, A. M. Annaswamy, and E. Lavretsky, “Adaptive control of hypersonic vehicles in the presence of rate limits,” in *2018 AIAA Guidance, Navigation, and Control Conference*, 2018, p. 0846.
- [31] R. S. Sutton, A. G. Barto, and R. J. Williams, “Reinforcement learning is direct adaptive optimal control,” *IEEE Control Systems*, vol. 12, no. 2, pp. 19–22, 1992.
- [32] S. Koos, J.-B. Mouret, and S. Doncieux, “Crossing the reality gap in evolutionary robotics by promoting transferable controllers,” in *Proceedings of the 12th annual conference on Genetic and evolutionary computation*, 2010, pp. 119–126.
- [33] J. Tan, T. Zhang, E. Coumans, A. Iscen, Y. Bai, D. Hafner, S. Bohez, and V. Vanhoucke, “Sim-to-real: Learning agile locomotion for quadruped robots,” *arXiv preprint arXiv:1804.10332*, 2018.

- [34] N. Fulton and A. Platzer, “Safe reinforcement learning via formal methods: Toward safe control through proof and learning,” in *Proceedings of the AAAI Conference on Artificial Intelligence*, vol. 32, no. 1, 2018.
- [35] A. Roy, H. Xu, and S. Pokutta, “Reinforcement learning under model mismatch,” *arXiv preprint arXiv:1706.04711*, 2017.
- [36] A. Rajeswaran, K. Lowrey, E. Todorov, and S. Kakade, “Towards generalization and simplicity in continuous control,” *arXiv preprint arXiv:1703.02660*, 2017.
- [37] C. Packer, K. Gao, J. Kos, P. Krähenbühl, V. Koltun, and D. Song, “Assessing generalization in deep reinforcement learning,” *arXiv preprint arXiv:1810.12282*, 2018.
- [38] Y. Nesterov, “A method of solving a convex programming problem with convergence rate $O(1/k^2)$,” *Soviet Mathematics Doklady*, vol. 27, pp. 372–376, 1983.
- [39] A. Krizhevsky, I. Sutskever, and G. E. Hinton, “Imagenet classification with deep convolutional neural networks,” in *Advances in Neural Information Processing Systems 25*. Curran Associates, Inc., 2012, pp. 1097–1105.
- [40] I. Sutskever, J. Martens, G. Dahl, and G. Hinton, “On the importance of initialization and momentum in deep learning,” in *Proceedings of the 30th International Conference on Machine Learning*, vol. 28, no. 3. PMLR, 2013, pp. 1139–1147.
- [41] K. S. Narendra and A. M. Annaswamy, *Stable Adaptive Systems*. NJ: Prentice-Hall, Inc., 1989, (out of print).
- [42] B. Anderson, R. R. Bitmead, C. R. Johnson Jr, P. V. Kokotovic, R. L. Kosut, I. M. Mareels, L. Praly, and B. D. Riedle, *Stability of Adaptive Systems: Passivity and Averaging Analysis*. MIT press, 1986.
- [43] G. Chowdhary, T. Yucelen, M. Mühlegg, and E. N. Johnson, “Concurrent learning adaptive control of linear systems with exponentially convergent bounds,” *International Journal of Adaptive Control and Signal Processing*, vol. 27, no. 4, pp. 280–301, 2013.
- [44] S. B. Roy, S. Bhasin, and I. N. Kar, “Combined MRAC for unknown MIMO LTI systems with parameter convergence,” *IEEE Transactions on Automatic Control*, vol. 63, no. 1, pp. 283–290, 2018.
- [45] R. Ortega, S. Aranovskiy, A. Pyrkin, A. Astolfi, and A. Bobtsov, “New results on parameter estimation via dynamic regressor extension and mixing: Continuous and discrete-time cases,” *IEEE Transactions on Automatic Control*, 2020.
- [46] A. Rantzer, “Concentration bounds for single parameter adaptive control,” in *2018 Annual American Control Conference (ACC)*. IEEE, 2018, pp. 1862–1866.
- [47] N. M. Boffi and J.-J. E. Slotine, “Implicit regularization and momentum algorithms in nonlinearly parameterized adaptive control and prediction,” *Neural Computation*, vol. 33, no. 3, pp. 590–673, 2021.

- [48] A. Astolfi and R. Ortega, “Immersion and invariance: a new tool for stabilization and adaptive control of nonlinear systems,” *IEEE Transactions on Automatic control*, vol. 48, no. 4, pp. 590–606, 2003.
- [49] J. E. Gaudio, A. M. Annaswamy, M. A. Bolender, E. Lavretsky, and T. E. Gibson, “A class of high order tuners for adaptive systems,” *IEEE Control Systems Letters*, vol. 5, no. 2, pp. 391–396, apr 2021.
- [50] J. E. Gaudio, A. M. Annaswamy, J. M. Moreu, M. A. Bolender, and T. E. Gibson, “Accelerated learning with robustness to adversarial regressors,” *3rd L4DC conference (to appear); arXiv preprint arXiv:2005.01529*, 2020.
- [51] S. McDonald, Y. Cui, J. E. Gaudio, and A. M. Annaswamy, “A high-order tuner for accelerated learning and control,” *arXiv preprint arXiv:2103.12868*, Mar. 2021.
- [52] J. M. Moreu and A. M. Annaswamy, “A stable high-order tuner for general convex functions,” *IEEE L-CSS (accepted for publication); arXiv preprint arXiv:2011.09996*, 2020.
- [53] B. D. Anderson and C. Johnson, “Exponential convergence of adaptive identification and control algorithms,” *Automatica*, vol. 18, no. 1, pp. 1–13, 1982.
- [54] G. C. Goodwin, P. J. Ramadge, and P. E. Caines, “Discrete time stochastic adaptive control,” *SIAM Journal on Control and Optimization*, vol. 19, no. 6, pp. 829–853, 1981.
- [55] J. E. Gaudio, T. E. Gibson, A. M. Annaswamy, M. A. Bolender, and E. Lavretsky, “Connections between adaptive control and optimization in machine learning,” *58th IEEE Conference on Decision and Control (CDC)*, 2019.
- [56] N. Matni, A. Proutiere, A. Rantzer, and S. Tu, “From self-tuning regulators to reinforcement learning and back again,” in *2019 IEEE 58th Conference on Decision and Control (CDC)*. IEEE, 2019, pp. 3724–3740.
- [57] T. Westenbroek, E. Mazumdar, D. Fridovich-Keil, V. Prabhu, C. J. Tomlin, and S. S. Sastry, “Adaptive control for linearizable systems using on-policy reinforcement learning,” in *2020 59th IEEE Conference on Decision and Control (CDC)*. IEEE, 2020, pp. 118–125.
- [58] R. Sun, M. L. Greene, D. M. Le, Z. I. Bell, G. Chowdhary, and W. E. Dixon, “Lyapunov-based real-time and iterative adjustment of deep neural networks,” *IEEE Control Systems Letters*, 2021.
- [59] S. M. Richards, N. Azizan, J.-J. E. Slotine, and M. Pavone, “Adaptive-control-oriented meta-learning for nonlinear systems,” *arXiv preprint arXiv:2103.04490*, 2021.
- [60] S. Dean, H. Mania, N. Matni, B. Recht, and S. Tu, “Regret bounds for robust adaptive control of the linear quadratic regulator,” *arXiv preprint arXiv:1805.09388*, 2018.
- [61] M. Fazel, R. Ge, S. Kakade, and M. Mesbahi, “Global convergence of policy gradient methods for the linear quadratic regulator,” in *International Conference on Machine Learning*. PMLR, 2018, pp. 1467–1476.

- [62] A. Guha and A. Annaswamy, “Mrac-rl: A framework for on-line policy adaptation under parametric model uncertainty,” *arXiv preprint arXiv:2011.10562*, 2020.
- [63] Y. Cui, J. E. Gaudio, and A. M. Annaswamy, “A new algorithm for discrete-time parameter estimation,” *arXiv preprint arXiv:2103.16653*, Mar. 2021.
- [64] Z. T. Dydek, A. M. Annaswamy, and E. Lavretsky, “Adaptive control of quadrotor uavs: A design trade study with flight evaluations,” *IEEE Transactions on control systems technology*, vol. 21, no. 4, pp. 1400–1406, 2012.
- [65] E. Lavretsky and K. A. Wise, *Robust and Adaptive Control with Aerospace Applications*. Springer London, 2013.
- [66] L. P. Kaelbling, M. L. Littman, and A. W. Moore, “Reinforcement learning: A survey,” *Journal of artificial intelligence research*, vol. 4, pp. 237–285, 1996.
- [67] J. Schulman, P. Moritz, S. Levine, M. Jordan, and P. Abbeel, “High-dimensional continuous control using generalized advantage estimation,” *arXiv preprint arXiv:1506.02438*, 2015.
- [68] A. M. Devraj and S. P. Meyn, “Zap q-learning,” in *Proceedings of the 31st International Conference on Neural Information Processing Systems*, 2017, pp. 2232–2241.
- [69] F. Berkenkamp, M. Turchetta, A. Schoellig, and A. Krause, “Safe model-based reinforcement learning with stability guarantees,” in *Advances in neural information processing systems*, 2017, pp. 908–918.
- [70] A. Loquercio, E. Kaufmann, R. Ranftl, A. Dosovitskiy, V. Koltun, and D. Scaramuzza, “Deep drone racing: From simulation to reality with domain randomization,” *IEEE Transactions on Robotics*, vol. 36, no. 1, pp. 1–14, 2019.
- [71] Y. Qin, M. Cao, and B. D. Anderson, “Lyapunov criterion for stochastic systems and its applications in distributed computation,” *IEEE Transactions on Automatic Control*, vol. 65, no. 2, pp. 546–560, 2019.
- [72] T.-H. Lee and K. S. Narendra, “Robust adaptive control of discrete-time systems using persistent excitation,” *Automatica*, vol. 24, no. 6, pp. 781–788, 1988.
- [73] J. Schulman, F. Wolski, P. Dhariwal, A. Radford, and O. Klimov, “Proximal policy optimization algorithms,” *arXiv preprint arXiv:1707.06347*, 2017.
- [74] S. Bubeck, “Convex optimization: Algorithms and complexity,” *Foundations and Trends in Machine Learning*, vol. 8, no. 3-4, pp. 231–357, 2015.
- [75] A. Annaswamy, C. Thanomsat, N. Mehta, and A.-P. Loh, “Applications of adaptive controllers to systems with nonlinear parametrization,” 1998.
- [76] J. E. Gaudio, A. M. Annaswamy, E. Lavretsky, and M. A. Bolender, “Parameter estimation in adaptive control of time-varying systems under a range of excitation conditions,” *IEEE Transactions on Automatic Control (submitted)*, 2020.

- [77] J. Duchi, E. Hazan, and Y. Singer, “Adaptive subgradient methods for online learning and stochastic optimization,” *Journal of Machine Learning Research*, vol. 12, pp. 2121–2159, 2011.
- [78] A. Somanath and A. Annaswamy, “Adaptive control of hypersonic vehicles in presence of aerodynamic and center of gravity uncertainties,” in *49th IEEE Conference on Decision and Control (CDC)*. IEEE, 2010, pp. 4661–4666.
- [79] M. Schwager and A. M. Annaswamy, “Direct adaptive control of multi-input plants with magnitude saturation constraints,” in *Proceedings of the 44th IEEE Conference on Decision and Control*. IEEE, 2005, pp. 783–788.

Anuradha Annaswamy is Founder and Director of the Active-Adaptive Control Laboratory in the Department of Mechanical Engineering at the Massachusetts Institute of Technology (MIT), Cambridge, MA, USA. Her research interests span adaptive control theory and its applications to aerospace, automotive, propulsion, and energy systems as well as cyber physical systems such as Smart Grids, Smart Cities, and Smart Infrastructures. Her research team of 15 students and post-docs is supported at present by the US Air-Force Research Laboratory, US Department of Energy, Boeing, Ford-MIT Alliance, and NSF. She has received best paper awards (Axelby; CSM), Distinguished Member, and Distinguished Lecturer awards from the IEEE Control Systems Society (CSS) and a Presidential Young Investigator award from NSF. She is the author of a graduate textbook on adaptive control, co-editor of two vision documents on smart grids as well as two editions of the Impact of Control Technology report, and a member of the National Academy of Sciences Committee study that published a report on the Future of Electric Power in the United States in 2021. She is a Fellow of IEEE and IFAC. She served as the President of CSS in 2020.

Anubhav Guha is a Masters student in the Active-Adaptive Controls Laboratory at MIT. His research interests and focus include adaptive control, reinforcement and machine learning, and robotics.

Yingnan Cui is a PhD student in the Active-Adaptive Control Laboratory in the Department of Mechanical Engineering at MIT. His research interests include adaptive control and optimization methods for machine learning.

Joseph Gaudio received his PhD degree in Mechanical Engineering from MIT in 2020. He is currently a Principal Engineer at Aurora Flight Sciences, a Boeing Company. His research interests are in adaptive control and machine learning.

José M. Moreu received the B.S. and S.M. degree in naval engineering from Universidad Politécnica de Madrid, Spain (2016 & 2018) and the S.M. degree in mechanical engineering from MIT in 2021. He worked in the Active-Adaptive Control Laboratory, Department of Mechanical Engineering, focusing on optimization methods for machine learning and adaptive control.